Historical Fermi All-Sky Variability Analysis of Galactic Flares

S. Joffre,[1] N. Torres-Albà,[1] M. Ajello,[1] D. Kocevski,[2] and R. Buehler[3]

[1]Department of Physics and Astronomy, Clemson University, Kinard Lab of Physics, Clemson, SC 29634, USA

[2]ST12 Astrophysics Branch, NASA Marshall Space Flight Center, Huntsville, AL 35812, USA

[3]Deutsches Elektronen Synchrotron DESY, D-15738 Zeuthen, Germany

ABSTRACT

The *Fermi* All-sky Variability Analysis (FAVA) provides a photometric alternative for identifying week-long gamma-ray flares across the entire sky while being independent of any diffuse Galactic or isotropic emission model. We reviewed 779 weeks of *Fermi*-LAT data analyzed by FAVA to estimate the rate and origin of Galactic gamma-ray flares, and to search for new variable Galactic gamma-ray transients. We report an estimated yearly rate of ∼ 8.5 Galactic gamma-ray flares/year with ∼ 1 flare/year coming from unknown sources. Out of the known gamma-ray sources that are spatially coincident with these detected flares, we report gamma-ray flares for six of them for the first time. All six are classified as pulsars, or a source of unknown nature but which positionally overlaps with known supernova remnants or pulsar wind nebulae. This potentially means these sites are tentative candidates to be the second known site of a variable gamma-ray pulsar wind nebula (PWN), after the famous Crab Nebula's PWN. Additionally, we identify 9 unassociated flares that are unlikely to have originated from known gamma-ray sources.

1. INTRODUCTION

Launched in June of 2008, the *Fermi Gamma-ray Space Telescope* regularly surveys the gamma-ray sky with the Large Area Telescope (LAT, Atwood et al. 2009). *Fermi*-LAT is able to observe the entire sky approximately every 3 hours. This semi-uniform exposure, as well as the LAT's stable instrument response, good angular resolution (< 0.15° at >10 GeV[1]), and large energy range (20 MeV − 2 TeV) have made *Fermi*-LAT an ideal instrument for studying time-varying phenomena in the gamma-ray sky.

Ongoing observations by the LAT have shown that the GeV sky is populated by transient sources whose gamma-ray flux varies on an assortment of timescales. Gamma-ray bursts (GRBs) and pulsars' high-energy flux can vary in as short as a fraction of a second (Ajello et al. 2019; Abdo et al. 2013). Day-long flux variations have been observed in the Crab Nebula (Abdo et al. 2010b; Balbo et al. 2011; Striani et al. 2011; Tavani et al. 2011) as well as in multiple novae (Cheung et al. 2016; Li et al. 2017b; Franckowiak et al. 2018; Nelson et al. 2019). Blazars have been observed to emit gamma-rays whose emission timescales can vary from days and weeks (Dinesh et al. 2023; Cutini et al. 2023; Pittori et al. 2023;

Brill 2023) to months or even years (Abdo et al. 2010c; Nolan et al. 2012; Collaboration 2015; Abdollahi et al. 2020; Peñil et al. 2022; Otero-Santos et al. 2023).

Observations of the transient gamma-ray sky are done across multiple domains and collaborations. Searches for extremely short flares (< 1 sec) like GRBs are performed onboard *Fermi*, refined on ground, and made publicly available quickly through the Gamma-ray Coordinates Network (GCN) notices[2]. Searches of transients on the 6-hour to 1 day timescales are performed manually on the ground by the *Fermi* flare advocates and delivered to the community via Astronomer Telegrams (ATel) and refereed publications (Ciprini & Fermi-LAT Collaboration 2012). Sources whose variability timescale spans months-to-years are discovered and published in *Fermi*-LAT catalogs (Abdo et al. 2010c; Nolan et al. 2012; Collaboration 2015; Abdollahi et al. 2020, 2022). As for flares with a typical duration of 1 week, these have been detected with the *Fermi* All-sky Variability Analysis (FAVA; Ackermann et al. 2013) and are reported in the first and second catalog of Flaring Gamma-ray Sources from FAVA (1FAV Ackermann et al. 2013, 2FAV Abdollahi et al. 2017).

The vast majority of all the variable sources discovered by *Fermi* are identified as blazars, a class of extremely

---

[1] Single photon, 68% containment radius

variable active galactic nuclei (Urry 1999). The very bright Galactic diffuse emission, which extends up to high Galactic latitudes and all along the Galactic plane, hampers the detection of Galactic transients. Ignorance of the sub-degree spatial structure of the Galactic diffuse emission coupled to systematic uncertainty in the LAT instrumental response (both the effective area and the point-spread function) makes source detection in the plane often difficult on all but the shortest (< 1s) timescales. This has strongly limited our knowledge of Galactic transients. Of the Galactic transients currently detected in gamma-rays (excluding pulsars and millisecond pulsars as they are a well-studied population, and their transient nature does not originate from flares), the following Galactic source populations are represented: gamma-ray binaries (Mirabel 2012), novae (Ackermann et al. 2014a), and the Crab Nebula's Pulsar Wind Nebula (PWN; Abdo et al. 2011). However, new detections even within these known source classes are rare. The Incremental *Fermi* Large Area Telescope Fourth Source Catalog Data Release 4 (4FGL-DR4, Ballet et al. 2023), only reports the firm identifications[3] of 11 binary systems, 8 novae[4], and 13 PWN. If we include associations[5], the total number of sources represented by these three source classes is 60. Galactic sources exhibiting transient behavior are even rarer. The Second Catalog of Flaring Gamma-ray Sources from the *Fermi* All-sky Variability Analysis (2FAVA; Abdollahi et al. 2017) reports 3 high-mass binaries (HMBs), 5 novae, and 1 PWN (the Crab). The detection of a new Galactic transient has the potential to add significantly to the current data set due to the low statistics of observed Galactic transients.

In this work, we utilized FAVA to identify transients at low-latitudes ($|b| < 10°$) that are likely to be of Galactic origin. We define the term 'flare' to be a FAVA detected transient occurring over a week-long period with a positive flux variation. A 'long-term flare' is defined to describe any set of spatially coincident FAVA flares that occur in consecutive weeks. We present our method, analysis, and results in the following manner:

---

[3] The 4FGL identification criterion depends on the source type. For pulsars or X-ray binaries they must find correlated periodic variability to be labeled as a 'firm identification'

[4] Not all novae detected by *Fermi*-LAT are reported in the 4FGL-DR4 due to the shorter duration of the flare. Koji Mukai's running list of all *Fermi*-LAT detected novae can be found here: https://asd.gsfc.nasa.gov/Koji.Mukai/novae/latnovae.html. As of June 2023, 18 have been detected.

[5] A Bayesian (spatial coincidence only) and a Likelihood Ratio (spatial with log N-log S) method are used for associations. See Section 5 of Abdollahi et al. 2020
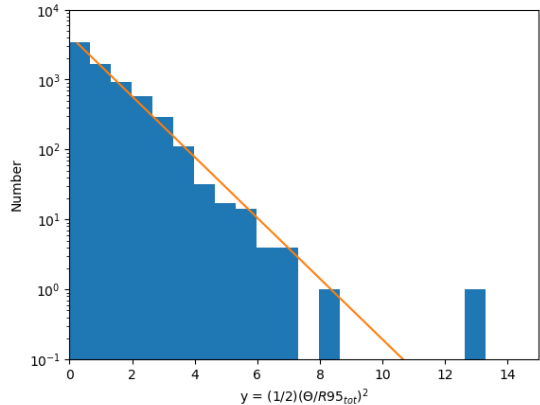

Figure 1. Best fit for calibration of $R_{95\%}$ values with Eqn. 2 plotted in log-log space. $f_{rel} = 1.06$

Section 2 reviews how the positional 95% uncertainty radius ($R_{95\%}$) was calibrated while Section 3 outlines how FAVA works and our selection criteria for flaring Galactic gamma-ray candidates. Following that, Section 4 outlines the properties of the flares coincident with Galactic gamma-ray sources, as well as with unassociated sources. Lastly, Section 5 and Section 6 review and summarize this work.

2. UNCERTAINTY RADIUS CALIBRATION

Currently, 1FAV and 2FAV include a 0.1° estimated systematic correction factor for a detected flare's uncertainty radius (Ackermann et al. 2013; Abdollahi et al. 2017). This systematic is based on the positions of known gamma-ray sources in comparison to the detected flares. Additional sources present in the 4FGL enable us to more accurately estimate the systematic uncertainty on a flare's positional. Following the method discussed at the end of Section 3.1.3 of the 4FGL paper (Abdollahi et al. 2020) we calibrated the maximum likelihood analysis method's derived $R_{95\%}$ uncertainty regions for the FAVA detected gamma-ray flares. First, we cross-matched the FAVA flares that were spatially coincident with a known 4FGL gamma-ray source, giving us 7069 flares. This number reflects the removal of all FAVA detections that reported a $R_{95\%}$ of 0.8°, which is the default value if the maximum likelihood analysis fails to converge properly. To estimate the systematic uncertainty we introduce a relative systematic factor f_{rel} such that

$$R_{95tot} = f_{rel} R_{95stat} \qquad (1)$$

where R_{95tot} is the total error (at the 95% confidence level) and R_{95stat} is the uncertainty error in the position.

Defining Θ as the angular separation between the FAVA detected source location and the counterpart lo-

cation of the source, we test various values of f_{rel} until the value y as defined by

$$y = \frac{1}{2}\left(\frac{\Theta}{R_{95tot}}\right)^2 \qquad (2)$$

follows a Rayleigh distribution (i.e. $exp(-y)$). Our best fit is achieved for $f_{rel} = 1.06$ and is plotted in Figure 1. Therefore, all reported $R_{95\%}$ have been increased by 6% over their original values reported by FAVA.

3. DATA SELECTION

All data was procured from the *Fermi* All-sky Variability Analysis (FAVA) website[6]. The last week of data reported in this paper is week 780 (July 17th, 2023).

3.1. *FAVA*

The *Fermi* All-sky Variability Analysis (FAVA; Ackermann et al. 2013) identifies transients across the entire sky using a photometric analysis method. In this method, FAVA does not rely on any Galactic diffuse model. Instead, FAVA assumes that the diffuse gamma-ray emission is constant over long time periods (> weeks). FAVA searches for transients by comparing measured counts over a week-long time bin at every point in the sky to the average emission over the first 4 years of the *Fermi* mission. FAVA does so while accounting for the difference in exposure time of the sky, and the point spread function (PSF) dependence on both energy and the instrument off-axis angle. Observed counts above this 4 year averaged emission are analyzed and are converted into a probability of a flare being present. All analysis on the week-long time bins is broken into two energy bands: a low energy band (LE; $100-800$ MeV) and a high energy band (HE; $800-300{,}000$ MeV). Abdollahi et al. 2017 reports a photometric LE flux sensitivity of $F_{LE} = 3.67 \times 10^{-7} \text{cm}^{-2}\text{s}^{-1}$ and a HE flux sensitivity of $F_{LE} = 3.24 \times 10^{-8} \text{cm}^{-2}\text{s}^{-1}$. To better localize the origin of the flare, a maximum likelihood analysis is performed at its position. For an in-depth explanation of this and FAVA please see Abdollahi et al. 2017.

Table 1. Cuts On FAVA Dataset For Determining Unassociated Flares

Cut Number	Cut Criterion	Number of Flares Cut	Number of Unassoc. Flares Remaining
1	FAVA Week $1-780$	0	24832
2	$|b| < 10°$	22622	2210
3	LE or HE Fava detection $> 5\sigma$	1380	830
4	Unassoc, Unassoc. and Gal. or no 4FGL coincidence	687	143
5	Coincident with 2FAV blazar	12	131
6	WISE IR blazar colors	120	11
7	Solar Vicinity	0	11
8	CHIME, BAT, BGM: Gamma-ray burst cross-match	1	10

Table 1

See Section 3.2 for a detailed description. For Cut 4, 105 flares are exclusively coincident with a known Galactic 4FGL-DR4 source or a gamma-ray emitting nova. Ten additional flares are spatially coincident with 1 or more Galactic 4FGL-DR4 source, or a gamma-ray emitting nova. All of these flares have a solar distance $> 16°$.

3.2. *Filter for Identifying Galactic and Unassociated Flare Candidates*

To minimize contamination in our data set from extragalactic sources the following cuts were made. The number of detected flares remaining after the cut is reported. Table 1 is a summary of the cuts utilized to identify the number of unassociated flaring Galactic gamma-ray candidates. We note that the $R_{95\%}$ used for the FAVA detected flare is from the localized maximum likelihood analysis of the flare where the HE or LE band is used depending on which one is better localized. We have calibrated these $R_{95\%}$ as discussed in Section 2.

1. All detected flares from the FAVA website from week 1 to week 780[7] (August 4th, 2008 − July

[7] Week 768 is excluded due to analysis complications from the FAVA pipeline so the data is not accessible.

17th, 2023) at a threshold of > 5[8] are downloaded[9] $- 24{,}832$ flares

2. All flares with a Galactic latitude $|b| < 10°$ are retained $- 2{,}210$ flares remain

3. Only flares whose low-energy and/or high-energy FAVA detection is at least 5σ are saved $- 830$ flares remain

4. The remaining flares are then positionally cross-matched with the 4FGL-DR4 (Ballet et al. 2023), Roma-BZCAT (Massaro et al. 2015) as well as the list of definitive gamma-ray emitting novae by Koji Mukai[10]. We break this down into 4 categories:

   - Flares positionally coincident with a 4FGL-DR4 blazar or a blazar reported in the Roma-BZCAT. These flares are removed.

   - Flares exclusively coincident with the position of a known 4FGL-DR4 Galactic source or a gamma-ray emitting novae (i.e. are not spatially coincident with an unassociated or known blazar source). These flares are set aside and are categorized as originating from known Galactic sources.

   - Flares positionally coincident with a 4FGL-DR4 unassociated source, or with a 4FGL-DR4 unassociated source and a known Galactic source

   - Flares that do not positionally coincide with a gamma-ray source reported in the 4FGL-DR4.

The 4FGL-DR4 does not provide gamma-ray $R_{95\%}$ for some of the detected novae, as well as not detecting others, hence, why we utilize the compiled gamma-ray novae list. This second subset (flares exclusively coincident with the position of a known 4FGL-DR4 Galactic source or a gamma-ray emitting novae) is composed of 105 individually unique FAVA flares. This subset is set aside and will be discussed at the end of this section. The last two items encompass possibly new, or unknown sources, and are the subset of flares we discuss for the remainder of the data selection cuts. $- 143$ flares

5. Flares that are coincident with a 2FAV source that is associated with a known blazar are eliminated $- 131$ flares remain.

6. Following the Wide-Field Infrared Survey Explorer (WISE) blazar strip as reported in Massaro et al. 2012, we developed a code[11] to filter out any flare detection whose $R_{95\%}$ contains a WISE source (from the AllWISE catalog) with infrared colors within the blazar strip in all 3 dimensions (W1$-$W2 vs. W2$-$W3, W2$-$W3 vs. W3$-$W4, and W1$-$W2 vs. W3$-$W4) as this is considered a likely blazar. Upper limits on reported AllWISE magnitudes are considered. $- 11$ flares remain.

7. FAVA reports the real-time angular distance of the flare to the position of the Sun at the time the flare was detected. Following Ackermann et al. 2013, since the Sun is a bright gamma-ray emitting source, we cut all flares whose Sun distance is less than 12°. None of these remaining flares met this criteria so none were cut $- 11$ flares remain.

8. Lastly, in order to see if the unassociated FAVA detected flares are coincident with other transient detections we cross-matched our remaining flares with the First Chime/FRB Fast Radio Burst catalog (CHIME/FRB Collaboration et al. 2021), the *Swift*/BAT Hard X-Ray Transient Monitor (Krimm et al. 2013), the Third *Swift* Burst Alert Telescope Gamma-Ray Burst (GRB) Catalog (Lien et al. 2016), the Fourth Fermi-GBM Gamma-Ray Burst Catalog (von Kienlin et al. 2020) and the *Fermi*-LAT catalog of long-term gamma-ray transient sources (1FLT; Baldini et al. 2021). The only spatial cross-matches that occur is with the Third *Swift* Burst Alert Telescope (BAT) Gamma-Ray Burst (GRB) Catalog, and the Fourth Fermi-GBM Gamma-Ray Burst Catalog. Both catalogs report the detection of GRB 221009A (RA: 288.26, DEC: 19.77; 2022 October 9 at 13:16:58.99 UTC (Lesage et al. 2023)) which is both spatially and temporally coincident with one of the 11 remaining unassociated FAVA flares (flare 7401). This GRB is the recently detected brightest-of-all-time (BOAT) GRB with the highest total isotropic-equivalent energy and highest fluence and peak flux GRB ever identified (Burns et al. 2023). Therefore, this flare is removed $- 10$ flares remain.

---

[8] This is not equivalent to a 5σ Gaussian significance. See the github page for notes

[9] See https://github.com/dankocevski/pyFAVA and Appendix for more details

[10] Included in the downloadable files for this paper.

[11] See https://github.com/tryingastronomy/Blazar_codes/tree/main/AW_blazar_strip and Appendix for more details

9. Flares that have coincident positions based on overlapping $R_{95\%}$ are assumed to be flaring events likely originating from the same source. Only two of the 10 unassociated flares spatially overlap. See Table 5 – We report 9 unique, new flaring objects of unknown origin.

Over almost 15 years of data, we find a total of 9 distinctly new flaring sources (composed of 10 flares) that have not been associated to any known gamma-ray detected source and are of potential Galactic origin (see Table 5). We find an additional 105 flares that are coincident with a single Galactic gamma-ray source, plus 10 flares that are coincident with more than one, resulting in a total of 115 flares coincident with at least 1 Galactic gamma-ray source (see Table 2). This means we have 125 flares of likely Galactic origin. Section 5.1 discusses the yearly flare rate more thoroughly.

The flares that are spatially associated with Galactic gamma-ray sources, novae, and unassociated flares are all outlined in three separate tables. Table 2 reports on non-novae concomitant with FAVA detections, Table 3 reports on the FAVA detections of classical novae, and Table 5 reports on FAVA flares that we propose as originating from unidentified Galactic transient sources.

3.3. Rate of Spurious FAVA Detections

Since we are selecting flares on a 5σ statistical significance, this leaves a margin for spurious detections. To evaluate the likelihood of one of our FAVA detected flares being spurious, we first calculate the total number of trials. The number of trials can be calculated using

$$N_{trials} = N_{weeks} \times N_{channels} \times N_{sky\,pixels} \quad (3)$$

where $N_{trials}, N_{weeks}, N_{channels},$ and $N_{sky\,pixels}$ all correspond to the number of trials, weeks, energy channels, and sky pixels used in the analysis, respectively. With $N_{weeks} = 779, N_{channels} = 2,$ and $N_{sky\,pixels} = 165,012$ where

$$N_{sky\,pixels} = \frac{\text{Total Sky}}{\text{Pixel}} = \frac{41,253\,\text{deg}^2}{0.25\,\text{deg}^2} = 165,012 \quad (4)$$

resulting in $N_{trials} = 257,088,696$. Since a 5σ detection corresponds to a probability $P = 3 \times 10^{-7}$, this means there is a 1/3,333,333 chance of a wrongful detection. Dividing our number of trials by 3,333,333 we expect 77 spurious FAVA detections out of 257,088,696 trials. From our 779 weeks analyzed, we find 13,218 flares were detected at a 5σ level, meaning we expect 0.5% of all FAVA detections to be false. Hence, we do not expect any of our vetted flares to be of spurious origin.

3.4. Background Extragalactic Contamination Estimates

Ackermann et al. 2013 found that by simulating extragalactic sources at low latitudes (after accounting for differences in solid angle and sensitivity corrections), 60% of low-latitude, variable extragalactic sources would be able to be detected by LAT. The 2FAV also reports a total of 323 flares at $|b| < 10°$, of which, 249 are associated to an extragalactic source. We therefore anticipate that of the 2,210 flares our investigation finds at $|b| < 10°$, 1701 are likely of extragalactic origin. After all of our cuts that were implemented to eliminate extragalactic contamination, we removed over 2,000 flares (with 125 Galactic gamma-ray flare candidates remaining). The number of removed flares means it is very likely that we have properly accounted for this potential contamination on a statistical basis.

3.5. Robustness of the 3D WISE blazar Strip

Filter criterion No. 6 in Section 3.2, the 3D WISE Blazar strip (W1−W2, W2−W3, W3−W4; Massaro et al. 2012), was tested using 1) 4FGL-DR4 blazars 2) 4FGL-DR4 Galactic sources, and 3) known Fermi-LAT detected gamma-ray novae

3.5.1. Testing Known Blazar Sources

The 4FGL-DR4 contains 3,934 blazars of the BLL, FSRQ, and undetermined type. In this catalog, the gamma-ray detection is reported as well as the associated counterpart, if known. Using the $R_{95\%}$ of the 4FGL-DR4 gamma-ray detection, we verify whether or not a WISE source contained therein has WISE colors that would place it within all three dimensions of the blazar strip. Of the 3,934 known blazars in the 4FGL-DR4, ~ 96% are compatible (considering the upper limits) with the blazar strip.

Of the known blazars, ~ 89% are at high latitude, ($|b| > 10°$). This leaves 420 known blazars at a latitude of $|b| < 10°$. Of the blazars that lie in the plane, ~76% are captured in all three dimensions of the blazar strip.

3.5.2. Testing Known Galactic Sources as reported by 4FGL-DR4

The 4FGL-DR4 reports 584 sources of Galactic origin (pulsars, supernova remnants (SNR), high mass binaries (HMBs), etc.). Of the reported Galactic sources, 405 occur at low latitudes ($|b| < 10°$). Of the known Galactic sources at low latitude (as some are at $|b| > 10°$), ~ 39% have uncertainty regions which contain a WISE source whose colors are consistent with a blazar. This means our method wrongly captures ~ 39% of low-latitude Galactic sources as blazars. Many of these WISE sources

report upper limits (i.e. the value of the magnitude is a minimum) for the different WISE filters. If one of the WISE source's color values has the possibility to fall in the blazar strip because of this limit, we count it as a possible blazar.

3.5.3. *Fermi-LAT Detected Gamma-ray Novae*

We also test Koji Mukai's compiled list of *Fermi*-LAT detected classical novae mentioned in the introduction. Of the 18 definitive detections (reported as of October 10th, 2023), only 10 have a WISE source within 5 arcseconds of the optically detected location. Out of these 10 sources, only 1 falls in all three blazar strips (V407 Cyg, which we detect with FAVA. See Table 3). Since we assume that the lack of a WISE source means that the source in question is not a blazar, then we only mistake gamma-ray novae for blazars 6% of the time.

3.5.4. *Sensitivity and Specificity of 3D WISE blazar Strip*

Since we are particularly interested in this test working at low latitudes ($|b| < 10°$) we report the results of low latitude sources reported in the 4FGL-DR4. For clarification:

- True positives (TP) are low latitude blazars flagged as blazars

- False positives (FP) are low latitude Galactic sources flagged as blazars

- True negatives (TN) are low latitude Galactic sources which have no WISE sources in their $R_{95\%}$ with colors consistent with blazars in all three dimensions of the WISE blazar strip. Therefore these are not flagged by the blazar strip (because they are not blazars).

- False negatives (FN) are low latitude blazars whose $R_{95\%}$ contains no WISE source with colors consistent with a blazar in all three dimensions of the WISE blazar strip. Therefore this blazar is not flagged by the blazar strip as a blazar.

Sensitivity, or true positive rate (TPR) is defined as

$$\text{TPR} = \frac{\text{TP}}{\text{TP} + \text{FN}} \quad (5)$$

while specificity, or true negative rate (TNR) is defined by

$$\text{TNR} = \frac{\text{TN}}{\text{TN} + \text{FP}} \quad (6)$$

For our purposes, sensitivity reflects the ability of the test to correctly identify a source as a blazar. Specificity, on the other hand, reflects the ability of the test

to identify non-blazar sources (i.e. Galactic sources). From the tests in Section 3.5.1 and Section 3.5.2 we find the following values

- TP = 318 blazars flagged as blazars

- FP = 159 Galactic sources flagged as blazars

- TN = 246 Galactic sources not flagged as blazars

- FN = 102 blazars not flagged as blazars

which results in a sensitivity (or TPR) of 75.7% and a specificity (TNR) of 60.7% . These values can be combined to determine the test accuracy (ACC)

$$\text{ACC} = \frac{\text{TP} + \text{TN}}{\text{TP} + \text{TN} + \text{FP} + \text{FN}} \quad (7)$$

which, when the above values are evaluated in equation 7 the result is ACC= 68.4%. The accuracy value reflects the fraction of blazars and Galactic sources which are properly flagged compared to the entire set that is analyzed.

4. RESULTS

4.1. *Overview of FAVA Flare Properties Coincident with Galactic Sources*

We find 115 FAVA-detected flares that are spatially coincident with at least 1 4FGL Galactic gamma-ray source, with 105 flares exclusively coincident (spatially) with a single Galactic source. We have determined that all 115 flares spatially coincide with only 19 known Galactic gamma-ray sources. Approximately ∼ 75% of the 105 flares that are spatially coincident with a single Galactic gamma-ray source can be attributed to Cygnus X-3, the Crab Nebula, and the high-mass binary (HMB) system of PSR B1259-63. See Section 4.3 for more discussion. Overall, the source types that are spatially coincident with a FAVA flare are: high-mass binary (HMB), Pulsar wind nebula (PWN), pulsar (PSR), nova (NOV), millisecond pulsar (msp), and potential association with supernova remnant or pulsar wind nebula (spp).

The sources reported in Table 2 are typically best fit with a `LogParabola` model in the 4FGL-DR4, but for the sake of comparison with the FAVA fits, we only report the power law fit for each source from the 4FGL. Additionally, we report the averaged FAVA LE and FAVA HE band indices from the FAVA detected flares that are spatially coincident with the 4FGL source. Out of the known Galactic sources detected by FAVA, the hardest spectrum reported by the DR4 is PSR B1259-63 with $\Gamma_{4FGL} = -2.33 \pm 0.27$. The hardest LE band source is the PSR J1826-1256 or SNR G018.1-00.1 at

−2.14 ± 0.28. Of flares spatially coinciding with a 4FGL Galactic source, the only flare detected at a > 5σ level in the HE band is PSR B1259-63.

Among the 18 known gamma-ray novae so far, using our selection criteria, 8 were detected by FAVA (see Table 3). These are V407 Cyg, V959 Mon, V1324 Sco, V339 Del, V5855 Sgr, V5856 Sgr, V906 Car, and V392 Per. Two of these novae had FAVA flares that were coincident with other sources. Flare Identification number (FID) 862, which we have identified as V407 Cyg, is also positionally coincident with SNR G085.9−00.6. But, due to the temporal coincidence during the height of the gamma-ray emission from V407 Cyg (see Abdo et al. 2010a), this flare most likely originated from the nova. Similarly, FID 4311, encompasses the positions of both V5855 Sgr and the blazar of uncertain type (bcu) NVSS J181120-275946. The Variability_Index (as reported by the 4FGL-DR4) of this blazar is 16.27, which falls below the threshold (27.69) at which the source has a 99% chance of being variable. This flare is detected in the same week that V5855 Sgr peaked in gamma-rays (Li et al. 2016; Li & Chomiuk 2016; Munari et al. 2017). We therefore conclude that this flare originated from V5855 Sgr.

Selecting the most significant detections from the novae with multiple detections, 6 novae were detected above 5σ in both LE and HE bins while the remaining 3 were detected only in the HE bin (see Table 3). No gamma-ray detected nova flares were detected exclusively in the LE bin. The average LE photon index of all of these novae is $\Gamma_{LE} = -1.49 \pm 0.39$, while the average HE photon index is $\Gamma_{HE} = -2.57 \pm 0.36$. The stark difference in slope between the LE and HE bin (being hard and soft, respectively) points to these novae emission peaking between the two bins. Since the dividing line is at 800 MeV, we expect that many of these gamma-ray detected novae are displaying a cutoff around a few GeV, which has been reported in previous analyses (Ackermann et al. 2014b; Metzger et al. 2016).

Table 2. DR4 Galactic Sources Coincident with FAVA Galactic Flare Candidates[†]

Associated Source	4FGL Name	DR4 Source Class[a]	LE σ*	HE σ*	Exclusive Flare Number[b]	Max Possible Flare Number[c]	Γ^d_{4FGL}	$\Gamma^f_{LE_{avg}}$	$\Gamma^f_{HE_{avg}}$
Cygnus X-3	4FGL J2032.4+4056	HMB	11.89	4.78	30	36	-2.68 ± 0.04♦	-2.52 ± 0.22	-2.56 ± 0.52
Crab Nebula (IC Field)	4FGL J0534.5+2201	PWN	23.56	4.29	28	...	N/A♦△	-3.38 ± 0.34	-2.26 ± 0.73
PSR B1259−63	4FGL J1302.9-6349	HMB	18.41	6.84	21	...	-2.33 ± 0.27	-2.83 ± 0.20	-2.17 ± 0.69
LSI +61 303	4FGL J0240.5+6113	HMB	7.08	2.49	7	8	-2.39 ± 0.005♦	-2.33 ± 0.27	-1.85 ± 0.64
PSR J0248+6021	4FGL J0248.4+6021	PSR	6.29	1.07	3	4	-2.64 ± 0.02▽	-2.96 ± 0.33	-3.01 ± 0.59
PSR J2032+4127	4FGL 2032.2+4127	PSR	8.51	3.97	2	8	-2.61 ± 0.01▽	-2.61 ± 0.19	-2.73 ± 0.56
PSR J1731-1847	4FGL J1731.7-1850	msp	5.01	-0.46	1	...	-2.65 ± 0.09♦	DNC×	DNC×
SNR G016.0−00.5[†]	4FGL J1821.4-1516	spp	5.55	4.03	1	...	-2.90 ± 0.09♦	-2.96 ± 0.32	-0.06 ± 0.78
SNR G016.7+00.1[†]	4FGL J1821.1-1422	spp	5.55	4.03	...	...	-2.66 ± 0.06♦	...	...
PSR J1826-1256[‡]	4FGL J1826.1-1256	PSR	9.66	1.04	1	...	-2.46 ± 0.01▽	-2.14 ± 0.28	-1.59 ± 0.54
SNR G018.1-00.1[‡]	4FGL J1824.1-1304	spp	9.66	1.04	...	...	-2.94 ± 0.09♦	...	...

Table 2

[a] Capitalized classifications are confirmed associations, lowercase are positionally coincident associations, high-mass binary (HMB), Pulsar wind nebula (PWN), pulsar (PSR), Nova (NOV), millisecond pulsar (msp), potential association with supernova remnant or pulsar wind nebula (spp)

[b] - Number of FAVA flares that are spatially coincident with only this Galactic source and no others.

[c] - Total possible number of FAVA flares that could have originated from this Galactic source, where we include flares that are coincident with this and at least 1 other DR4 known Galactic source. '...' corresponds to the maximum number being the same as the Exclusively Coincident Flare Number

[d] - 4FGL-DR4 reported power law photon index

[f] - Average photon index of all FAVA flares exclusively coincident with the source listed.

[†] - These Galactic sources are spatially coincident with the same flare, FID 3472

[‡] - These Galactic sources are spatially coincident with the same flare, FID 3473. Two additional unassociated 4FGL sources are also coincident with the edge of the flare: 4FGL J1826.5-1202c and 4FGL J1828.1-1312

♦ - 4FGL-DR4 best fit as LogParabola

△ - 4FGL-DR4 does not report a power law fit for the inverse Compton emission of the Crab PWN. It is fit with a LogParabola model with LP.Index = 1.75 and LP.beta = 0.08.

▽ - 4FGL-DR4 best fit as PLSuperExpCutoff

* - Highest detection recorded. Note, may not be the same flare for LE σ and HE σ column

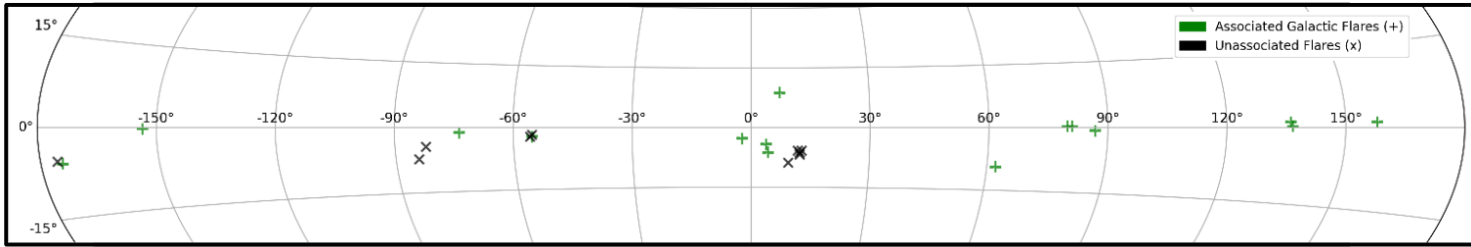× - Follow-up maximum likelihood analysis did not converge (DNC)

Figure 2. Sky distribution of detected flares. A single exclusively coincident FAVA flare that is spatially associated with a Galactic gamma-ray source or nova from Table 2 and Table 3 is represented by one of the 15 green crosses (as 4 sources are non-exclusive with the spatially coincident flare their flares are not included). The 10 black 'X's correspond to the 10 unassociated Galactic flare candidates in Table 5.

Table 3. Gamma-ray Novae Coincident with FAVA Galactic Flare Candidates

Name	Date of γ-ray Peak[a] Y/M/D	Paper/ATel	Ang. Sep[b] (°)	FAVA $R_{95\%}$[c] (°)	FAVA Dates of Detection Y/M/D	FIDs[d]	LE σ	HE σ	Γ_{LE}	Γ_{HE}
V407 Cyg	2010/3/13-14	Abdo et al. 2010a	0.12	0.08	2010/3/11-22	**843**,853,862	5.64*	10.27*	-1.37 ± 0.25*	-2.52 ± 0.20*
V959 Mon	2012/06/22 - 6/24	Cheung et al. 2012b	0.06	0.16	2012/6/18-25	2033	7.39	8.27	-1.82 ± 0.23	-3.33 ± 0.43
V1324 Sco	2012/6/15 - 7/2	Cheung et al. 2012a	0.06	0.07	2012/6/18-25	2034	4.15	6.43	-1.17 ± 0.33	-2.54 ± 0.24
V339 Del	2013/08/16	Hays et al. 2013	0.07	0.08	2013/8/12-19	26314, **26423**	8.73*	10.76*	-1.25 ± 0.22*	-2.54 ± 0.24*
V5855 Sgr	2016/10/28-11/1	Li & Chomiuk 2016	0.31	0.80	2016/10/31 - 11/7	4311	4.71	5.22	DNC	DNC
V5856 Sgr	2016/11/8	Li et al. 2016	0.22	0.80	2016/11/7-14	43231	6.82	14.64	DNC	DNC
V906 Car	2018/4/10-4/14	Aydi et al. 2020	0.09	0.04	2018/4/16-30	**5071**,5082	19.05*	24.76*	-1.81 ± 0.09*	-2.62 ± 0.09*
V392 Per	2018/4/30-5/8	Albert et al. 2022	0.04	0.07	2018/4/20 - 5/7	5091	4.55	6.38	-0.55 ± 0.76	-2.19 ± 0.22

Table 3
[a] Date as given by corresponding paper or ATel (Astronomer's Telegram)
[b] Average angular separation between the optically detected Novae location and the FAVA detected flare. Rounded up to hundreths of degree
[c] If multiple flares, the best (smallest) localized $R_{95\%}$ is reported
[d] Bolded text indicates the FID corresponding to the most significant detection (in both bands)
* Corresponds to the flare of highest significance

4.2. Associated Galactic Sources Detected by FAVA With Previous Flaring Behavior

In the following subsections, we outline our findings of flaring behavior for the number of sources previously known to vary that are spatially coincident with FAVA flares. Furthermore, we outline the previously understood flaring nature of these sources. We reiterate, the term 'flare' is meant to be a FAVA detected flare occurring over a week-long period unless otherwise noted. A 'long-term' flare is meant to describe any set of spatially coincident FAVA flares that occur in consecutive weeks.

4.2.1. Cygnus X-3

In this investigation, we report 30 FAVA flares exclusively coincident (spatially) with this source, and 6 additional flares that are also coincident with PSR J2032+4127. In this investigation we find Cygnus X-3 to have the highest number of coincident FAVA detected flares out of any known Galactic gamma-ray source. Of these 30 week-long flares, 10 occur in 2020 while 9 occur in 2021, with a total of 7 long-term flares.

Cygnus X-3 is a high-mass binary and the first microquasar detected by Fermi-LAT (Fermi LAT Collaboration et al. 2009). Composed of a neutron star or black hole (Koljonen & Maccarone 2017), this is one of the few binaries of this type where the donor star is a Wolf-Rayet star (van Kerkwijk et al. 1992). Furthermore, Fermi LAT Collaboration et al. 2009 found Cygnus X-3 to have a 4.8 hour orbital period. Recent work done by Prokhorov & Moraghan 2022 used a variable-size sliding-time-window (VSSTW) analysis to detect 23 intervals of 28-day windows where Cygnus X-3's gamma-ray emission was detected at levels $> 4\sigma$.

In 2021, 4 FAVA detected flares occur consecutively, from 2021 May 17 to 2021 June 14, likely detecting a single long-term flare. We find that in 2020, the 10 flares do not happen all consecutively, with the longest long-term flare happening from 2020 August 24 to 2020 September 14 (3 weeks). Prokhorov & Moraghan 2022 also reports a single long-term flare between 2020 April 27 and 2020 September 14. Lastly, Prokhorov & Moraghan 2022 reports the detection of a long-term flare from Cygnus X-3 during 14 September 2020 to 12 August 2021. FAVA detects 11 (non-consecutive) flares during this time.

4.2.2. Crab Nebula (PWN)

Coming in second for the most FAVA flares spatially coincident with a Galactic gamma-ray source, this investigation reports 28 spatially coincident FAVA flares with the Crab Nebula. Long-term flares are detected three times.

One of the most well-studied gamma-ray sources on the sky, the Crab, is composed of a pulsar at its center surrounded by a nebula and the scattered remains of the supernova that occurred in 1054 A.D. (Minkowski 1942). Even before the first FAVA catalog paper (Ackermann et al. 2013), gamma-ray flares from the Crab Nebula had been observed (Abdo et al. 2011; Tavani et al. 2011; Buehler et al. 2012). Abdo et al. 2011 identified a 16 day flare and 4 day flare in February 2009 and September 2010, respectively. Later, Striani et al. 2013 proposed the transient gamma-ray nature of the Crab to come from flares (above-average flux on the order of hours) and 'waves' (above-average outbursts occurring on the order of 1-2 weeks), the latter being formed by plasma instabilities with enhanced magnetic fields. Striani et al. 2013 records 7 different wave events from AGILE and Fermi-LAT data, 1 of which corresponds to 1 of our 28 FAVA flares that are exclusively coincident with the Crab. Labeled $W6$ in Striani et al. 2013, this wave-natured flare is reported to have lasted 12 days from 2012 March 02 to 2012 March 14. The temporally coincident FAVA detection occurred in the week from 2012 March 05 to 2012 March 12.

4.2.3. PSR B1259−63

We find 21 FAVA flares to be exclusively coincident with the high-mass binary system PSR B1259−63, with all flares being part of 4 individual long-term flares.

PSR B1259−63 is a pulsar that is part of a HMB system, with a massive B2e or Oe star companion (Wang et al. 2004; Aharonian et al. 2005; H. E. S. S. Collaboration et al. 2020). This source has a well reported orbital period of ∼ 1237 days, with an eccentricity of $\epsilon = 0.87$ (Wang et al. 2004). Prior to, and after periastron, PSR B1259−63 traverses the disk-like outflow of its partner star, with the disruption causing emission from radio to TeV energies. See Johnson et al. 2018 for a robust description of the system. The crossings were observed by Fermi-LAT, with the gamma-ray emission typically peaking ∼ 40 − 60 days after periastron in 2010 (Abdo et al. 2011; Tam et al. 2011), 2014 (Caliandro et al. 2015) 2017 (Chang et al. 2018; Johnson et al. 2018; Tam et al. 2018), and 2021 (Chernyakova et al. 2021). The official dates for the previous periastrons of this source are reported as: 2010 December 14 16:39:03 UTC, 2014 May 4 10:02:22 UTC, 2017 September 22 03:25:41, and 2021 February 9 20:48:59 UTC.

The 21 flares detected by FAVA that are exclusively coincident with this source follow the delayed gamma-ray emission of the disk crossing. The gamma-ray flares detected by FAVA in multi-week epochs are as follows: two 5-week long-term flares (2011 January 17 to 2011 February 21 and 2017 October 30 to 2017 December 4), one 4-week long-term flare (2014 June 2 to 2014 June
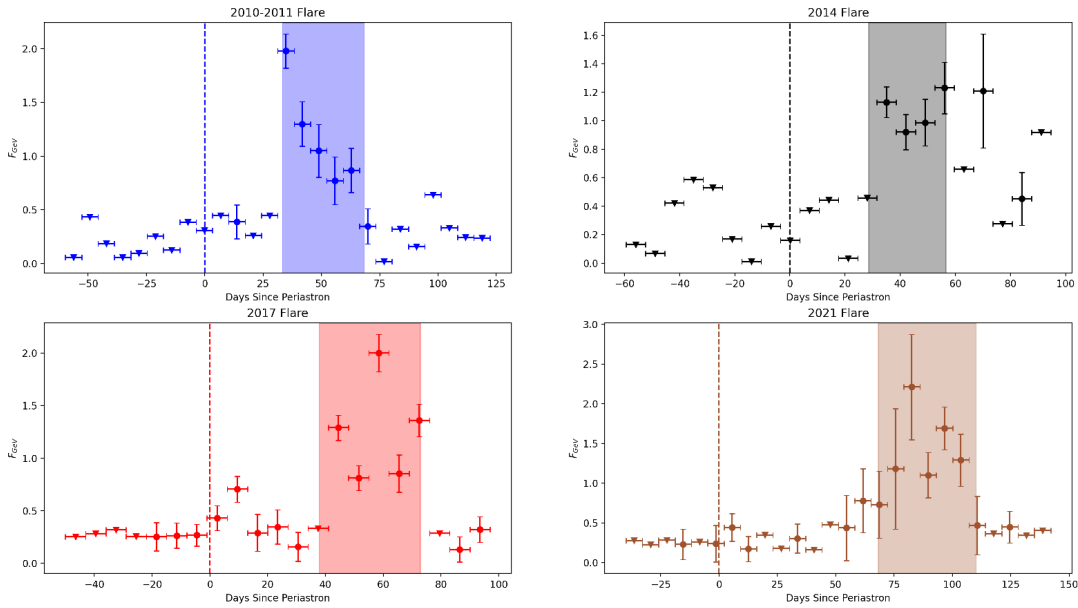
Figure 3. Adapted from Figure 1 in Chernyakova et al. 2021. F_{GeV} is the *Fermi*-LAT detected photon flux for $E > 100$ MeV in units of 10^{-6} photons/cm^2/s plotted against the number of days since periastron of PSR 1259-63. The dashed vertical line indicates point of periastron and highlighted regions are the consecutive weeks in which FAVA detected a significant long-term flare spatially coincident with this source.

30), and one 7-week long-term flare (2021 April 19 to 2021 May 31). Figure 3 is adapted from Chernyakova et al. 2021 which plots the *Fermi*-LAT flux over time. We have added highlighted bands indicating the consecutive weeks of detection by FAVA. Overall, FAVA accurately captures the peak gamma-ray emission as detected by *Fermi*-LAT.

Prokhorov & Moraghan 2022 also reports multi-week flaring behavior of PSR B1259−63 in gamma-rays, with a 5 week detection starting on 2017 October 25, and therefore overlapping with one of the long-term FAVA detections of this source.

4.2.4. *LS I +61 303*

LS I +61 303 is coincident with 7 flares exclusively, with no detections in consecutive weeks.

LS I +61 303 is another HMB system, with either a black hole or neutron star and a large Be star. One of the first sources whose orbital periodicity was detected in gamma-rays, LS I +61 303 has a 26.6 ± 0.5 day orbital period (Abdo et al. 2009). Others propose that LS I +61 303 could be, a magnetar (see Torres et al. 2011; Suvorov & Glampedakis 2022). Nonetheless, the object is known to be transient in gamma-rays. FAVA only detected this source on 7 occasions, and only in the 2009-2019 decade (but not in consecutive weeks).

4.3. *Associated Galactic Sources Detected by FAVA With No Previous Flaring Behavior*

This section focuses on sources that we report to be flaring in gamma-rays for the first time. In each case, a Galactic gamma-ray source with no known history of gamma-ray flaring behavior was found to be positionally coincident with at least one of the FAVA-detected flares. These sources are PSR J0248+6021, PSR J2032+4127, PSR J1731−1847, SNR G016.0-00.5, SNR G016.7+00.1, PSR J1826-1256, and SNR G018.1-00.1.

4.3.1. *PSR J0248+6021*

Our investigation finds a total of 4 flares coincident with the pulsar PSR J0248+6021, 3 of which are solely coincident with this source. Although Theureau et al. 2011 detected a series of short bursts above the average signal strength of the pulsar, these bursts occurred in radio frequencies and on time periods analogous to the pulsar's spin period of 217 ms.

The First Large High Altitude Air Shower Observatory (LHAASO) is a TeV air shower detector composed of a Water Cherenkov Detector Array (WCDA) and the Kilometer Squared Array (KM2A) (Cao et al. 2023). The First LHAASO Catalog of Gamma-ray Sources (1LHAASO) reports persistent TeV sources. LHAASO's WCDA data came from 2021 March 05 to 2022 September 30, while KM2A detections are reported from 2020 January to 2020 to September. Two of the three FAVA-detected flares exclusively coincident with this pulsar occurred in weeks during the time period of the 1LHAASO catalog. Although the 4FGL-DR4 does not report a TeV flag from previous TeV telescopes, both

LHAASO detectors report a TeV source coincident with PSR J0248+6021. 1LHAASO J0249+6022 is detected by KM2A (RA, DEC: 42.39, 60.37; $R_{95\,stat}$ = 0.40°, Γ_{KM2A} = 3.82 ± 0.18) with a significance of TS=148.8 and by WCDA (RA, DEC: 41.52, 60.49; $R_{95\,stat}$ = 0.16°, Γ_{WCDA} = 2.52±0.16) at TS=53.3. The position of these sources in comparison to PSR J0248+6021 is seen in Figure 4. We note that $\Gamma_{4fgl}, \Gamma_{LEavg},$ and Γ_{HEavg} all are in agreement with Γ_{WCDA} within 1σ (see Table 2).

1LHAASO proposes that the TeV source corresponds to an astrophysical system associated with PSR J0248+6021 (e.g a composite SNR). Therefore, we propose that our FAVA detected flares are the first week-long detected gamma-ray outbursts involving PSR J0248+6021 and a neighboring system, or nearby feature such as a nebula.
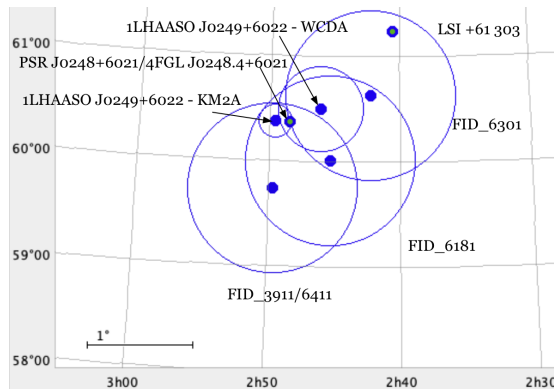
Figure 4. FAVA flare positions and $R_{95\%}$ along with LHAASO source positions and statistical $R_{95\%}$ that are coincident with PSR J0248+6021. Nearby 4FGL sources are also labeled.

4.3.2. *PSR J2032+4127*

With two exclusively coincident flares, the pulsar PSR J2032+4127 also provides an interesting potential location of gamma-ray flares. In 2017, the pulsar was identified to be in a binary system with a 15 $M_\odot$ star (Ho et al. 2017). With the pulsar displaying X-ray brightening (Ho et al. 2017). Li et al. 2017a conducted long-term X-ray observations and found week-long variability embedded in the long-term increasing trend. Li et al. 2018 conducted studies with *Fermi*-LAT but did not detect variability at GeV energies.

Due to the vicinity of a nearby TeV source, Abeysekara et al. 2018 used the Major Atmospheric Gamma Imaging Cherenkov telescope (MAGIC; Bigongiari 2005) and the Very Energetic Radiation Imaging Telescope Array (VERITAS; Holder et al. 2006) to observe PSR J2032+4127 in which they detected gamma-ray emission rising to a factor of 10 above baseline before quickly

dropping off a week later. These results led PSR J2032+4127 to be the second TeV gamma-ray binary system to be detected with the compact object nature known. Abeysekara et al. 2018 model the low state and high state of the outburst as a power law plus a baseline component. The MAGIC detection of the outburst has a best fit of $\Gamma_{MAGIC\,low}$ = 2.57 ± 0.26 and $\Gamma_{MAGIC\,high}$ = 2.17 ± 0.23, with the low state index agreeing with the LE and HE average indices detected by FAVA (see Table 2)

These MAGIC/VERITAS observations occurred during periastron (2017 November 13) and do not correspond with the coincident FAVA flares. Six other FAVA flares that are coincident with PSR J2032+4127 are also coincident with Cygnus X-3, so additional analysis is necessary to know if the two flares exclusively coincident with PSR J2032+4127 should actually be attributed to Cygnus X-3. If they are from PSR J2032+4127, these flares would be the first GeV energy flares detected by this source at these week-long timescales. The *Fermi* Light Curve Repository (LCR; Abdollahi et al. 2023) reports a heightened flare state in weekly time bins for Cygnus X-3 during both flares that are coincident only with PSR J2032+4127 (FID 6012 and 6911). Therefore, we find it likely that these originate from Cygnus X-3, but further analysis is required to confirm this.

4.3.3. *PSR J1731−1847*

PSR J1731−1847, a millisecond pulsar (msp), is spatially coincident with a single source. This millisecond pulsar is identified to be an eclipsing binary, but this effect would only delay the timed pulses on the order of fractions of a second (Bates et al. 2011). We note that the typical likelihood analysis done by FAVA to better localize this source failed to converge (and therefore giving a $R_{95\%}$ of 0.8°), and we recommend future analysis in order to identify the origin of this flare, as it could potentially be indicative of the msp interacting with its neighboring environment (i.e. a flaring PWN). If further analysis identifies this to be the origin of the flare, it would be the first gamma-ray flare reported from this millisecond pulsar's environment.

4.3.4. *Flares Coincident with Multiple Galactic Sources Not Known to Flare*

There are two more flares which may have originated from a flaring PWN, but are coincident with more than one non-variable Galactic gamma-ray source. The two flares are:

1. FID 3472 - found spatially coincident with SNR G016.0-00.5 and SNR G016.7+00.1

2. FID 3473 - found spatially coincident with PSR
   J1826-1256 and SNR G018.1-00.1.

See Table 2 for additional details on these 4FGL sources and their coincident FAVA flares. We note that both of these FAVA-detected flares were detected in the same week, and within about 1.86° from one another. FID 3473 was also reported in 2FAV and was labeled as unassociated since the flare could not be firmly established to have originated from PSR J1826-1256 alone. All known Galactic sources that are spatially coincident with these flares are classified as spp, except PSR J1826-1256 (a known pulsar, see Table 2). Since the origin of the spp sources is currently ambiguous, we will not discuss them in particular. In order to better understand the nature of these detected flares a robust LAT analysis needs to be applied for the week these flares were detected. However, due to the presence of multiple potential PWN, this environment could potentially host a flaring PWN.

4.4. *Potential Crab-Like PWN*

Above we discussed the potential association of FAVA flares to pulsars, and possible PWN - both of these environments could potentially mean a flaring PWN is present. Due to the flaring state of Cygnus X-3 during the weeks flares were found coincident with PSR J2032+4127, we find it likely that those flares originate from Cygnus X-3 (which is known to be variable, see Section 4.2.1).

We therefore propose that 4 separate flaring events (FID 3472, 3473, 6181, and 41136), which are positionally coincident with 6 different Galactic gamma-ray sources, could potentially originate from a flaring PWN. None of the coincident sources are reported as variable in the 4FGL-DR4. The Variability Index reported in the 4FGL-DR4 for SNR G016.0-00.5, SNR G016.7+00.1, PSR J1826-1256, SNR G018.1-00.1, PSR J0248+6021, and PSR J1731-1847 is 12.78, 4.00, 8.95, 14.78, 8.14 and 14.66, respectively. Since the 4FGL uses monthly binning for its light curves and this would only be a single week-long outburst at most, we find it unlikely to be detected in the 4FGL analysis. Although the follow-up likelihood analysis that is automatically done by FAVA converged (in most cases) for these flares, the $R_{95\%}$ of FID 3473 and 3472 are on on the order of ~ 40 arcminutes (< 0.8 deg). Detailed LAT analysis of all of these flares in their respective time windows while implementing improvements to the analysis (e.g. pulsar gating) may enable the identification of the origin of these flares.

Therefore, if any of these known gamma-ray sources are the origin of the flare, this would be the first reported gamma-ray flare reported from any of the sources. More importantly, if this flare originates from a PWN, that would make this flare the second variable PWN ever detected in gamma-rays. The only other PWN known to be variable in gamma-rays is the one surrounding the Crab nebula (Bühler & Blandford 2014).

4.5. *Overview of Unknown/Unassociated FAVA Flare Properties*

Out of the 10 individual unassociated flaring events that survived the cuts we implemented in Section 3, two of them (FIDs 55913 and 55822) positionally overlap, likely originating from the same source. The distribution of our 10 flares on the Galactic plane is depicted in an Aitoff projection in Figure 2.

With a selection criteria of a 5σ detection in either the photometric FAVA HE or LE band, we find that 5 unassociated flares are detected exclusively in the LE band (FID 55913, 1281, 6101, 6631, 72921), 1 exclusively in the HE band (FID 57924), and 4 are detected in both bands (FID 55822, 14127, 56019, 60334). See Table 5. The follow-up likelihood analysis implemented in FAVA, with our calibration of its calculated $R_{95\%}$, gives a more accurate $R_{95\%}$ than the photometric localization method alone. Additionally, the maximum likelihood analysis gives an estimation of the photon index of the flare in each band. The smallest $R_{95\%}$ (including our calibration) is 0.011° (FID 55822) and the largest is 0.270° (FID 60334), with a median value of ~0.05° across all detections. The mean photon index of all of the LE band detections (> 5σ for LE) is -2.31 ± 0.05 (of the 5 detected exclusively in this band, the mean is -2.47 ± 0.08). For all the HE-detected flares, the mean photon index in this band is -3.11 ± 0.15 (FID 57924, which is detected exclusively in the HE band, has a HE index of -2.61 ± 0.34). The distribution of photon indices of the unassociated flares, compared against the fitted power law photon index (Γ) of Galactic sources reported in the 4FGL-DR4 are presented in Figure 5.

4.5.1. *Kolmogorov-Smirnov and Anderson-Darling Tests*

In order to help determine if the unassociated Galactic flare candidates likely come from a source population that differs from the known Galactic or blazar sources, we implemented both Kolmogorov-Smirnov (KS) and Anderson-Darling (AD) statistical tests. Using the spectral indices calculated for the flares, we separate the flares into three subcategories: 1) flares spatially coincident with known Galactic sources, 2) flares spatially coincident with known blazar sources, and 3) unassociated flares. Each of these flaring source categories is then split into HE or LE detections. When there is more than one flare spatially coincident with a given source,
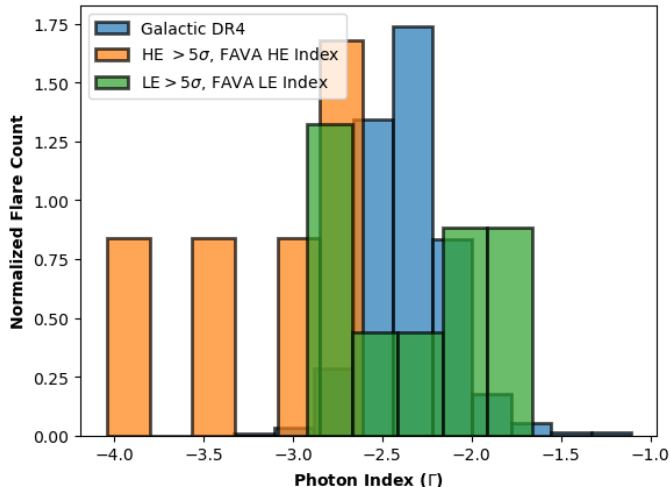
Figure 5. Distribution of power law spectral indices from the likelihood analysis reported by FAVA for our reported unassociated Galactic flaring candidates detected in the HE band (orange) or LE band (green). This is compared with the steady-state average power law fits for identified Galactic sources in the 4FGL-DR4 (blue). Note, most DR4 Galactic sources have their best fit with a `LogParabola` model but for comparison we plot the fitted power law values.

for each energy band we use the most significantly detected flare in that band. For the unassociated subsets, we only select flares if they have a $> 5\sigma$ detection. We then run KS and AD statistical tests on all of the combinations of source subsets and energy selected subsets.

Table 4 outlines the results of these two tests, with the p-value results of the AD test above the diagonal of 1's with KS calculated values below. Two major takeaways should be considered. Firstly, when testing the subsets with the LE detected unassociated flares, for both the AD and KS tests, the LE blazar flares have a higher p-value than the LE Galactic flares. In either case, the null hypothesis (unassociated sources come from a Galactic, or, blazar population) cannot be rejected.

Secondly, when tested with the HE unassociated flares, the HE Galactic flares have a higher p-value than the HE blazar flares, and in both tests the HE blazars have p-values < 0.02. This indicates that unassociated flares detected in the HE band are likely not from a blazar parent population.

4.6. *Potential Counterparts of Unassociated Sources*

In an effort to help identify the origin of the unassociated FAVA detected flares reported in Table 5, we utilized multiple X-ray source catalogs (Living *Swift*-XRT Point Source Catalog (LSXPS, Evans et al. 2023), the Fourth XMM-Newton Serendipitous Source Catalog, Thirteenth Data Release (4XMM-DR13, Webb et al. 2020), the Chandra Source Catalog (CSC, Evans et al. 2010), and *Swift*-BAT 105 month Catalog (Oh et al. 2018) as well as analyzed stacked archival data at the flare positions to determine persistent X-ray sources spatially coinciding with the FAVA detected flare. Most of the FAVA detected flares did not have contemporaneous X-ray data. The usage of archival X-ray data implies that we may miss the X-ray counterpart to the flares (if there was one). Therefore, all sources listed in the Appendix should only be taken as possible persistent counterparts.

In short, of the unassociated flares, 3 flares are coincident with 4XMM sources (FID 55913, 60334, 72921), 3 flares are coincident with LSXPS sources (FID 57924, 60334, 72921), 1 flare is coincident with a CSC source (FID 14127), and 3 flares are coincident with the *Swift*-BAT 105 month catalog (FID 14127, 55822, 55813). We note that, the coincident BAT detections are already associated to nearby blazars or the Crab Nebula. None of the persistent X-ray sources spatially coincident with one of our Galactic flaring candidates are reported to be transient in their respective catalogs. For a more in-depth description of the X-ray catalogs and the fields of each unassociated FAVA detected Galactic candidate, please see the Appendix.

4.6.1. *Flares that lack X-ray Data*

Beyond the X-ray catalogs, the High Energy Astrophysics Science Archive Research Center (HEASARC; Nasa High Energy Astrophysics Science Archive Research Center (Heasarc) 2014) was also searched for possible X-ray data (from *Swift*-XRT, *XMM*, *Chandra*, and *NuSTAR*) at the location of each of these FAVA detected flares. Three of the flares detected by FAVA have no archival X-ray data from the above mentioned missions. These flares are FID 1281, 6631, and 6101.

JOFFRE ET AL.

Table 4. KS and AD p-value Results

	Gal. LE	Gal. HE	Blz. LE	Blz. HE	Unassoc. LE	Unassoc. HE
Gal. LE	1		0.407		0.5105	
Gal. HE		1		0.0695		0.1925
Blz. LE	0.4348		1		0.7025	
Blz. HE		0.04372		1		0.0125
Unassoc. LE	0.5732		0.7904		1	
Unassoc. HE		0.121		0.009243		1

Table 4

Values are calculated with `ks.test` and `ad_test` from R. Values above the diagonal of 1's are the Anderson-Darling calculated p-values, while below are the Kolmogorov-Smirnov values. Only matching bands are compared.

Table 5. Unassociated FAVA Detected Galactic Flare Candidates[a]

Flare ID	RA (°)	DEC (°)	$R_{95\%}$ [C] (°)	LE σ [b]	HE σ [c]	LE Γ [d]	HE Γ [e]	Start Date M/D/Y	End Date M/D/Y	Closest 4FGL [f]	4FGL [g] Class	Dist/$R_{95\%}$ [h]
						Multiple[i]						
55822	278.46	-21.05	0.011	40.0*	40.0*	-2.12 ± 0.03	-2.93 ± 0.08	04/08/19	04/15/19	J1833.6-2103	FSRQ	4.1
55913○	278.46	-21.05	0.024	25.8	3.7	-2.25 ± 0.04	-2.29 ± 0.87	04/15/19	04/22/19	J1833.6-2103	FSRQ	1.7
						Single[j]						
1281	194.81	-65.46	0.058	7.5	1.5	-2.73±0.25	-1.03±0.48	01/10/11	01/17/11	J1302.9-6349	HMB	28.6
6101	138.01	-56.99	0.040	12.2	3.7	-1.66±0.06	-2.98±0.19	04/06/20	04/13/20	J0904.9-5734	bcu	28.2
6631	196.71	-64.75	0.169	10.2	0.6	-2.79±0.16	-0.81±0.48	04/12/21	04/19/21	J1302.9-6349	HMB	6.0
14127	83.69	22.01	0.014	40*	10.3	-2.06±0.03	-4.04±0.29	04/11/11	04/18/11	J0534.5+2200	Crab Pulsar	4.1
56019	278.49	-21.1	0.019	40*	40*	-1.81±0.03	-2.63±0.07	04/22/19	04/29/19	J1833.6-2103	FSRQ	4.1
57924	135.95	-57.61	0.104	3.0	5.5	-2.52 ± 0.38	-2.61 ± 0.34	09/02/19	09/09/19	J0904.9-5734	bcu	1.42
60334	278.25	-21.36	0.270	10.7	7.4	-2.44 ± 0.2	-3.36 ± 0.57	2/17/2020	2/24/2020	J1833.6-2103	FSRQ	1.24
72921	278.43	-20.81	0.077	5.6	0.3	-2.92 ± 0.29	-1.99 ± 0.49	07/18/22	07/25/22	J1833.6-2103	FSRQ	3.3

Table 5

[a] All FAVA reported associations for these detected flares listed 'None'
[C] Calibrated $R_{95\%}$ (i.e. scaled by 1.06. See Section 2)
[b] Significance of detection for $E = 100 - 800$ MeV. The maximum possible value is 40σ
[c] Significance of detection for $E = 800 - 300000$ MeV. The maximum possible value is 40σ
[d] Fitted power-law index for $E = 100 - 800$ MeV
[e] Fitted power-law index for $E = 800 - 300000$ MeV
[f] Source in the 4FGL closest to the FAVA detected flare by angular separation. All sources listed officially have the identifier '4FGL' prior to the listed name. All sources listed have a Variability Index > 27.69 as reported by the 4FGL-DR4
[g] Class designations listed are reported from the 4FGL-DR3 [h] Ratio of the angular separation distance between the nearest 4FGL source and the $R_{95\%}$ as reported by FAVA's follow-up localization, rounded to the nearest tenth.
[i] For clarity, the detections that likely originate from the same source are grouped together
[j] All flares listed in this section were not coincident with any other
* Is hitting the maximum significance threshold as reported by FAVA, and so could be higher.
○ - Ratio distance < 4 and *Fermi* Light Curve Repository reports a heightened state of the nearby 4FGL source

5. DISCUSSION

Due to the bright Galactic diffuse emission, as well as the systematic uncertainty, *Fermi*-LAT is biased against detecting flaring sources in the Galactic plane. In this work we used 14.98 years of data (779 weeks) to study the population of Galactic gamma-ray transients.

The 4FGL-DR4 only reports firm associations for 32 sources classified as gamma-ray binaries, novae, and PWN. With so few known Galactic sources detected in gamma-rays (we exclude millisecond pulsars in our discussion since the transient nature caused by their fast rotation is well studied), and even fewer of these source classes exhibit transient behavior (9 as reported by Abdollahi et al. 2017), this investigation uses *Fermi*-LAT All-sky Variability Analysis (FAVA) to identify potential Galactic candidates that would flare on week-long time periods.

After FAVA identifies flares with its photometric method, it also does an additional likelihood analysis of the detected flares, reporting spectral properties along with a better localized position ($< 0.8°$). For the unassociated flares that we posit to be Galactic flare candidates (see Table 5), of the flares detected exclusively in the HE band, the mean of the HE photon index is $\Gamma_{HEavg} = -2.40 \pm 0.28$ and of those detected exclusively in the LE band, the average LE photon index is $\Gamma_{LEavg} = -2.47 \pm 0.19$. Of the 4 flares detected with $> 5\sigma$ significance in both bands, their average HE index is $\Gamma_{both\,HE} = -3.24 \pm 0.16$ and their average LE index is $\Gamma_{both\,LE} = -2.11 \pm 0.05$. This seems to indicate that for these unassociated flares, when significantly detected in both bands they are generally harder in the LE band and softer in the HE band compared to the flares detected in a single energy band. Comparatively, the average photon index for a Galactic source reported in the 4FGL-DR4 is $\Gamma_{Galactic\,4FGL} = -2.33 \pm 0.01$, with PWN having the hardest average, ($\Gamma_{PWN} = -2.08 \pm 0.02$) and novae having the softest ($\Gamma_{NOV} = -2.46 \pm 0.06$).

We draw specific attention to FID 1281, 6631, and 6101 as each of these flares was significantly detected and occurred at a location in the sky with absolutely no archival X-ray observations. We highly recommend that these regions be systematically searched in follow-up campaigns to identify possible counterpart candidates to the origin of the FAVA detected flare. Although possibly coincidental, we note that each of these flares were all detected by FAVA in the LE and not the HE band (at $\geq 5\sigma$).

5.1. *Estimating Flare Rates of Galactic Origin*

We find 115 flares to be coincident with at least 1 known Galactic gamma-ray source. Additionally we fil-

tered the unassociated flares (as detailed in Section 3.2) to remove blazars. Our filter for selecting likely Galactic candidates, is able to correctly vet blazars from our data set with an accuracy of 68.4% (based on the use of the WISE blazar strip alone). Our testing of the WISE blazar strip gave us a false negative rate (FNR = 100 - TPR) of 24.3% and a false positive rate (FPR = 100 - TNR) of 39.3%. Filtering flares based on sources in their $R_{95\%}$ with the WISE blazar strip resulted in 10 individual flares remaining. Based on positional coincidence, we posit that these 10 flares originate from 9 distinct flaring Galactic candidates.

The false negative rate allows us to estimate that 2-3 of our 10 unassociated flares are potentially produced by blazars. In tandem with our estimates of possible wrongful identifications (see Section 5.2) we estimate the detection of 9 unassociated likely Galactic gamma-ray transients. Moreover, our false positive rate means that we likely filter out $3-4$ additional flaring Galactic candidates that were detected by FAVA.

We then estimate that over the course of the 779 weeks studied, 12-13 unassociated Galactic flares occurred. Combining these unassociated flares with the 105 FAVA flares coincident with only a single Galactic gamma-ray source as reported in the 4FGL-DR4, we estimate a total of 117-118 flaring events that are likely of Galactic origin during our time of study. If we count FAVA flares that coincide with more than one known Galactic gamma-ray source, this estimate becomes 127-128. Employing the estimate from all coincident FAVA and 4FGL-DR4 Galactic sources, along with likely Galactic candidates from this work, we estimate that there are ~ 8.5 Galactic gamma-ray transient events per year. Of those 8.5 flares, this exploration has led to the estimate that each year, ~ 1 of those comes from an unassociated flare, ~ 1 originates from a classical nova, ~ 2 are from Cygnus X-3, ~ 2 stem from the Crab Nebula, with the other ~ 2.5 coming from other Galactic gamma-ray sources.

5.2. *Likely Misidentified Detections and Most Likely Sources of Galactic Origin*

Some unassociated flares fall in the vicinity of nearby 4FGL sources (typically blazars). We want to establish whether, statistically, a flare would likely be caused by a nearby variable source. We establish a 'ratio distance' by taking the ratio of the distance from the flare to the nearest 4FGL source with the FAVA reported $R_{95\%}$ (i.e. dist/$R_{95\%}$). In essence, this establishes how many σ apart the two locations are - as in, how much disagreement their positions have. If the σ is large, it means that the flare is unlikely to have originated from the nearby source. On the other hand, if σ is small, it

means that the flare potentially could have originated from that nearby source. For the purposes of identifying the most promising flares, we establish a ratio distance of ≥ 4 as the cutoff for flares that are likely not a misidentified detection of the nearby source (since their distance apart compared to their localization is large). That is, the nearby 4FGL source has a ~0.006% chance of being of the same origin as the detected flare based on statistical properties alone.

Furthermore, if the nearby source has a a Variability Index > 27.69 as reported in the 4FGL, it has < 1% chance of being a steady source (Ballet et al. 2023; Scargle et al. 2013). Four of our FAVA detected Galactic flare candidates reported in Table 5 are at a ratio distance of < 4. Each of these four detected flares, the closest 4FGL source is likely variable. We suspect that these may be misidentified as new detections and are likely a flare caused by the nearby source.

Moreover, we checked these four unassociated FAVA Galactic flare candidates suspected of having originated from a their nearby 4FGL source by checking the closest 4FGL source in the *Fermi* Light Curve Repository (LCR; Abdollahi et al. 2023) using weekly time bins. FSRQ PKS 1830-211 (the closest 4FGL source to FID 55913) was flaring from a low to high state in one of its strongest flares recorded during the same week as FID 55913. For FID 57924, the nearest 4FGL source is PKS 0903-57 (a bcu) and during the week of the FAVA detected flare this blazar is slightly above the baseline variation, but not in a distinctively flaring state. PKS 1830-211, which is also the nearest 4FGL source for FID 60334, according to the LCR this source is actually in a decaying state from a large flare that occurred in late December of 2019. Lastly, PKS 1830-211 (also the nearest source for FID 72921) is at a relatively stable state during the week of FID 72921's detected flare. Overall this leads us to believe that FID 55913 is most likely a flare originating from the blazar, but the other three (FID 57924, 60334, 72921) could still potentially be from an unknown source. Therefore, we warn readers that FID 55913 is likely a flare from a blazar.

6. SUMMARY

Outside of the large number of pulsars detected at high-energies, only three other Galactic source classes are known to emit gamma-rays in a transient manner: gamma-ray binaries, novae, and the Crab Nebula Pulsar Wind Nebula. Of these source classes, the 4FGL-DR4 only reports persistent gamma-ray emission from 32 firmly identified sources (60 associated sources). Moreover, low statistics of Galactic gamma-ray transients for each of these source classes means the discovery of each

additional Galactic gamma-ray transient adds substantially to the statistics of the source class it belongs to.

As part of utilizing FAVA to identify new Galactic gamma-ray transients, we have been able to:

- Estimate a yearly Galactic gamma-ray transient rate of ~ 8.5 flares/year. The composition of this yearly rate is ~ 2 flares from the Crab Nebula, ~ 2 flares from Cygnus X-3, ~ 1 flare from a classical nova, ~ 1 unassociated source, with the remaining ~ 2.5 flares coming from other known Galactic gamma-ray sources.

- Report the first gamma-ray flare spatially coincident with 6 4FGL sources with no prior gamma-ray outbursts. These are: PSR J0248+6021, PSR J1731-1847, SNR G016.0-00.5, SNR G016.7+00.1, PSR J1826-1256, and SNR G018.1-00.1. SNR G016.0-00.5, SNR G016.7+00.1, and SNR G018.1-00.1 are all classified as either a supernova remnant, or a pulsar wind nebula. PSR J0248+6021, PSR J1731-1847, and PSR J1826-1256 are all pulsars. If follow-up analysis confirms that the flare does originate from one of these source environments, it would potentially mean the confirmation of a flaring pulsar wind nebula (PWN), and possibly the discovery of the second gamma-ray variable PWN like the Crab Nebula's PWN.

- Determine 10 individual unassociated flares that are of likely Galactic origin.

- Use the WISE blazar strip for filtering out possible blazars based on infrared counterparts in their gamma-ray $R_{95\%}$. Furthermore, we tested the WISE blazar strip using the gamma-ray locations and $R_{95\%}$ of sources reported in the 4FGL. We report the WISE blazar strip to have a 68% accuracy rate for correctly distinguishing blazars and Galactic sources given their gamma-ray detections. We also verify that classical novae with gamma-ray emission are unlikely to be filtered out (94% are not identified as blazars).

- Report 18 long-term flares (>1 week) from consecutive, coincident FAVA detections. These 18 long-term flares likely come from 4 unique Galactic gamma-ray sources. We expect at least 1 long-term flare per year to be detected by FAVA.

- Potential observational confirmation of the Crab Nebula's PWN 'wave' outburst behavior predicted by Striani et al. 2011.

- Identify spectral parameters for each unassociated flare. We find that, on average, when compared

to other unassociated flares detected in a single band, unassociated flares detected significantly in both LE and HE bands tend to be harder in the LE and softer in the HE. The mean photon index for all the unassociated flares detected in the LE band is -2.34 ± 0.23 and for all unassociated flares detected in the HE band is -2.44 ± 0.43.

- Report (in the Appendix) persistent X-ray sources from archival data that are spatially consistent with the FAVA detected flares. The potential Galactic flaring candidates with a persistent X-ray source coincident with their $R_{95\%}$ are FID 14127, 55822, 55813, 55913, 57924, 60334, and 72921.

- Recommend fields for future X-ray study since they had no X-ray observations where a likely flare of Galactic origin was detected. These flares are FIDs 1281, 6631, and 6101.

Future follow-ups and analysis of the fields with FAVA detected gamma-ray flares of likely Galactic origin could lead to the detection of new transient sources. Most importantly, it could verify a potentially new variable PWN.

Software: Astropy (The Astropy Collaboration et al. 2013), numpy (Harris et al. 2020), R (R Core Team 2023), SAO Image DS9 (Joye & Mandel 2003), TOPCAT (Taylor 2005), XSPEC (v12.11.1; Arnaud 1996)

APPENDIX

A. CODES

- Code used to webscrape data from the FAVA website: https://github.com/dankocevski/pyFAVA

- 3D WISE blazar strip checking AllWISE sources in $R_{95\%}$ with upper limits included: https://github.com/tryingastronomy/Blazar_codes/tree/main/AW_blazar_strip

B. X-RAY CATALOG DESCRIPTIONS

We cross-matched our 10 unassociated flares using the best $R_{95\%}$ from the maximum likelihood analysis of the FAVA detected flare with various X-ray catalogs. The catalogs are described below.

B.1. *Swift-BAT 105 Month Catalog*

Using $2.6'$ for *Swift*-BAT's $R_{95\%}$[12], we find 3 flaring Galactic candidates coincident with the *Swift*-BAT 105 month catalog. These are SWIFT J0534.6+2204 (Crab nebula) with flare 14127, SWIFT J1833.7-2105 (PKS 1830-21) with flares 55822 and 55913. These cross-matches, and the other possible counterparts for each FAVA detected Galactic flaring candidate are discussed in detail in Section C.

B.2. *LSXPS*

The Living *Swift*-XRT Point Source (LSXPS; Evans et al. 2023) catalog updates its collection of point sources detected by *Swift*-XRT in real time. LSXPS covers 5,371 deg^2, and when used for this manuscript was updated

---

[12] see   https://heasarc.gsfc.nasa.gov/docs/heasarc/caldb/swift/docs/bat/SWIFT-BAT-CALDB-CENTROID-v2.pdf

through 2023 October 25. LSXPS includes a method for detecting transients. This is done by 1) determining if it is a cataloged X-ray source, and 2) compares the measured flux to the source's historic upper limits. See Section 4 of Evans et al. 2023 for more details. Cross-matching our FAVA detected flares with the LSXPS transient catalog found no matches that were spatially coincident with one another. We note that a lack of X-ray monitoring over the fields of interest rather than the non-transient nature of the X-ray sources may be the cause of no cross-matches being detected.

B.3. *4XMM-DR13*

The Fourth XMM-Newton Serendipitous Source Catalog, Thirteenth Data Release (4XMM-DR13; Webb et al. 2020), released 2023 June 12, includes 13,243 XMM-Newton EPIC observations from 2000 February 3 − 2022 December 31, covering over 1328 $\deg^2$ of the sky. The 4XMM-DR13 also includes a `SC_VAR_FLAG` for the most variable detection of a source, `SC_Fvar` which reports the lowest probability that the source is constant, and `SC_chi2prob` which is the χ^2 probability that the unique source detected by one of the previous observations is constant. Out of the 54 sources that are spatially compatible with an unassociated FAVA flare, none were flagged as variable.

B.4. *CSC 2.0*

The *Chandra* Source Catalog 2.0 (CSC; Evans et al. 2010, 2020) includes 317,167 unique compact and extended X-ray sources detected by *Chandra* up until December 31, 2014. One of the 10 unassociated flaring Galactic source candidates are coincident with at least 1 *Chandra* detection (FID 14127).

C. POSSIBLE COUNTERPARTS AND X-RAY ANALYSIS IN THE FIELD OF FAVA DETECTED GALACTIC FLARES

For the 10 Galactic flaring candidates, 7 have archival X-ray data taken near the location of the detected event. Below, we outline potential counterpart candidates to the FAVA detected Galactic flaring candidates, starting with what we find in their X-ray fields. For those lacking X-ray data, we also discuss the known sources within each flare's $R_{95\%}$ that are reported by SIMBAD (Wenger et al. 2000). We recommend X-ray surveys of all areas of the sky covered by our flares, especially the fields that lack any X-ray observation. It is very possible that the individual counterpart responsible for the gamma-ray flare detected by FAVA is not detectable with the limited archival X-ray data we used. Since the X-ray observations do not coincide temporally with the FAVA detected flare, these reported counterpart candidates are simply the best counterpart candidates we have available at this time.

C.1. *Flare ID: 55913, 55822*

Flare 55913 and flare 55922 are coincident with one another. The nearest 4FGL object is the FSRQ, 4FGL J1833.6−2103. This variable object has been associated with the *Swift*-BAT detection, SWIFT J1833.8−2103 which is coincident with both flares. The ratio distance (distance to 4FGL object divided by FAVA detected $R_{95\%}$) is 1.7σ and $4.1\ \sigma$ for the different flares. As discussed above, FID 55913 likely is a misidentified flare that likely originates from this blazar.

C.2. *Flare ID 1281*

Flare 1281 is a ratio distance of 28.6σ away from the high mass binary (HMB), 4FGL J1302.9-6379, the nearest 4FGL source, which can be completely excluded as the counterpart based on distance alone. No archival X-ray data is present for this field. SIMBAD reports a few sources coincident with the FAVA detected flare, including a classical Cepheid variable, a spectroscopic binary, a RR Lyrae Variable, and a couple Long-Period Variable stars. None of these sources are convincing counterpart candidates to be the origin of a $100-800$ MeV flare. We recommend future studies of this region of the sky to identify the origin of this 7.5σ LE flare.

C.3. *Flare ID 6101*

The nearest 4FGL source is the blazar, 4FGL J0904.9-5734, at a ratio distance of 28.2σ. This large of a ratio means that this source can be excluded as the source of the flare. Flare 6101 also lacks X-ray observations in its $R_{95\%}$. Searching in SIMBAD only gives stars coincident with the position of the flare. Detected with a 12.2σ significance in the LE band and 3.7σ significance in the HE band, follow-up observations are necessary to properly study the origin of this flare.
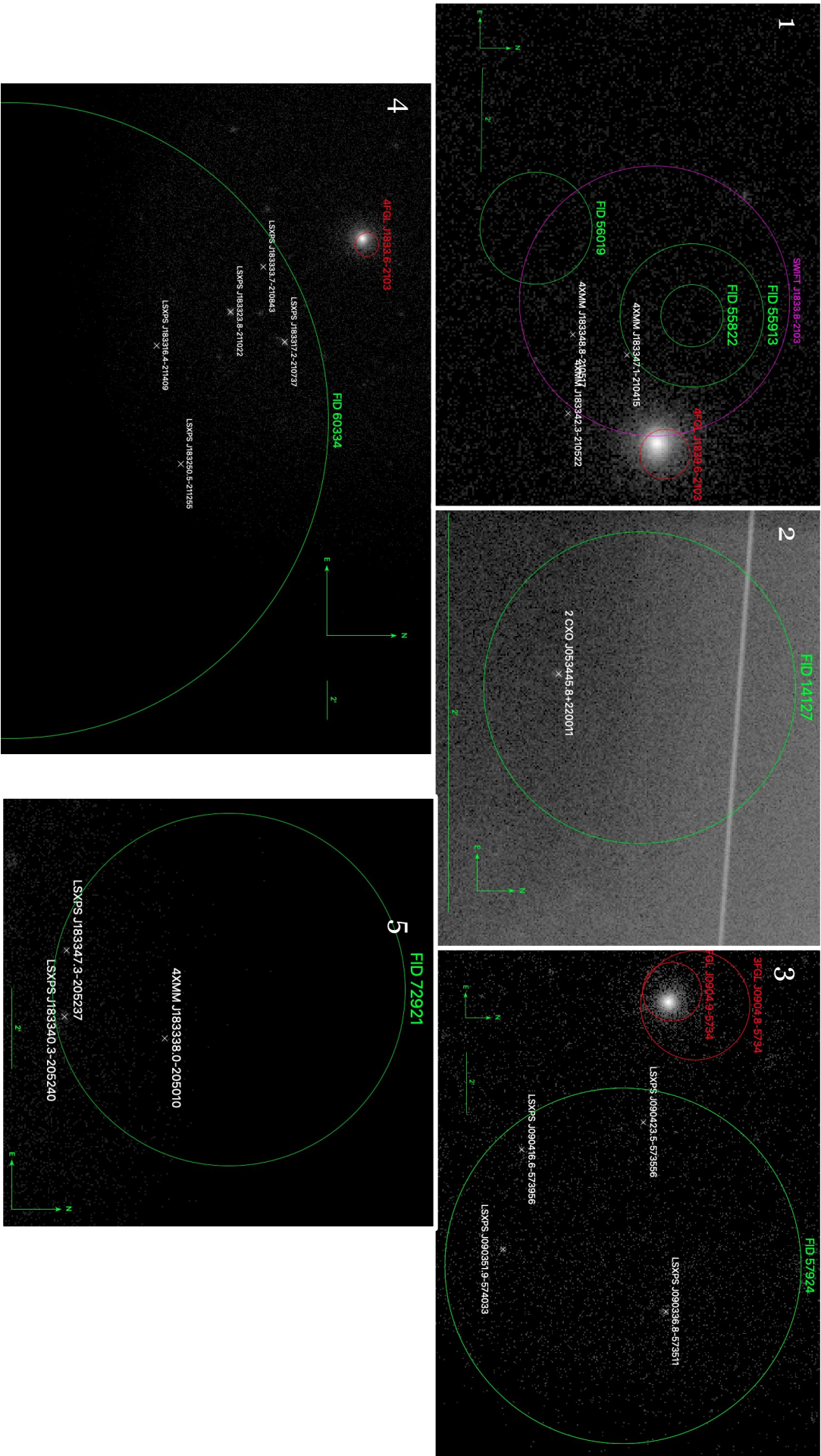
JOFFRE ET AL.

Figure 6. FAVA detected flares with X-ray data in the same FOV are plotted here with their corresponding FAVA detection (green), nearby 4FGL sources (red), 4XMM and LSXPS survey sources (white), and *Swift*-BAT coincident sources (magenta). All fields were observed using *Swift*-XRT (with the exception of Panel 2 which was observed with *Chandra*). FIDs 1281,6101, and 6631 lack X-ray data. FID 7401 is not included since it corresponds to GRB 221009A .

C.4. *Flare ID 6631*

In the neighborhood of flare 1281, FID 6631's detected flare's nearest known 4FGL neighbor is also 4FGL J1302.9-6379, with a ratio distance of 6.0σ. No X-ray data from *Swift*-XRT, *XMM*, or *Chandra* is available in the region of flare 6631. SIMBAD reports a multitude of stars of various types, but no object that would be a convincing counterpart to this significantly detected flare. Follow-up surveys of this region are required to discuss the possibilities of the origin of this flare more in depth.

C.5. *Flare ID 14127*

Detected on the outskirts of the Crab Nebula, flare 14127 is a ratio distance of 4.13σ to the pulsar at the center of the Crab's position. The ratio distance to the nearest point in the Crab's nebula (as detected in X-rays) is 2.24σ. The FAVA detected flare occurs well outside of the Crab Nebula itself. Checking the *Fermi* LCR, (which only reports the nebula's synchrotron component) the Crab's PWN has an increase in its flux between 2011 April 8 - 15, going from $7.97\pm1.78\times10^{-7}$ to $1.74\pm0.17\times10^{-6}$ photons/cm^2/s in the 0.1-100 GeV band. The average photon flux for the Crab PWN as reported through December 1, 2023 from the LCR is $1.26\times10^{-6}\pm1.1\times10^{-11}$ photons/cm^2/s . Although this week is above the mean value, it is not a dramatic departure. This, paired with the distance to the edge of the Crab points to this being a potential detection of a new source.

Flare 14127 has a $R_{95\%}$ that has minimal overlap with the uncertainty area of the *Swift*-BAT detection of the nebula (SWIFT J0534.6+2204). Within the FAVA detected flare's $R_{95\%}$, there is a CSC source present. 2CXO J053445.8+220011 was detected on January 27, 2004 at 5.87σ.(Evans et al. 2010, 2020). Although detected in 2004, no other observations of this part of the sky have been observed. Therefore, at this time the Chandra detected X-ray source appears to be the most likely candidate for the origin of the FAVA detected flare. We recommend further studies of this X-ray source, and this field to solidly confirm the origin of this flare.

C.6. *Flare ID 56019*

Occurring in the same region of the sky as FIDs 55913, and 55822 FID 56019 was detected in both the HE and LE bands at a significance of 40σ (the highest value that FAVA reports). With a ratio distance of 4.1σ from the nearby source, 4FGL J1839.6-2103, FID 56019 likely originates from a uniquely different source than FIDs 55913 and 55822. No persistent X-ray sources were spatially coincident with this detection

C.7. *Flare ID: 57924*

The $R_{95\%}$ of flare 57924 does not overlap with, but is nearby 4FGL J0904.9−5734, the highly variable (Variability Index = 8488.27) BL Lac object, although it was not flaring during the week of this FAVA detected flare. The ratios of distance to the nearest 4FGL source divided by the FAVA $R_{95\%}$ is 1.42. This flare has 4 LSXPS sources spatially coincident with its position.

Searching HEASARC, this flare has both archival *Swift*-XRT and *Chandra* data in the neighborhood of the flare. For the *Chandra* observation, we find the detected flares to be outside of the field of view (FOV). The most significant detection from the LSXPS J090336.8−573511 which is coincident with flare 57924 has a signal-to-noise ratio (SNR) of SNR=5.5. LSXPS J090351.9-574033 was detected at SNR = 3.9.

C.8. *Flare ID 60334*

With the largest $R_{95\%}$ out of the unassociated flares, the distance to the nearest 4FGL source divided by the $R_{95\%}$ is only 1.24. The nearest 4FGL source is the FSRQ, 4FGL J1833.6−2103. This 4FGL source has a variability of 37330 reported in the DR4, but is not varying during the week of the flare. Only part of the $R_{95\%}$ of FID 60334 has X-ray data with a number of LSXPS point sources. Since only a small portion of the $R_{95\%}$ area has been observed it is hard to determine if there is a proper persistent X-ray counterpart. This flare has 41 spatially coincident 4XMM sources and 15 LSXPS sources.

C.9. *Flare ID 72921*

The closest detected 4FGL source to this flare is 4FGL J1833.6−2103 at a ratio distance of 3.3. Falling on the outskirts of the *Swift*-XRT FOV, only a small portion of the FAVA $R_{95\%}$ has counts. Even in this small area of the $R_{95\%}$, multiple sources from LSXPS and 4XMM-DR12 are present. Two of the detections overlap and coincide with the same source, those being LSXPS J183340.3−205240 and 4XMM J183340.2−205241. Due to the lack of observation

of the entire FAVA detection, until additional observations are taken of this region, these persistent X-ray sources are our only counterpart candidates. This source has 4 spatially coincident 4XMM sources, and 2 from LSXPS.

REFERENCES

Abdo, A., Ackermann, M., Ajello, M., et al. 2011, Science, 331, 739

Abdo, A. A., Ackermann, M., Ajello, & Fermi LAT Collaboration. 2010a, Science, 329, 817, doi: 10.1126/science.1192537

Abdo, A. A., Ackermann, M., Ajello, M., et al. 2009, ApJL, 701, L123, doi: 10.1088/0004-637X/701/2/L123

—. 2010b, Science, 331, 739, doi: 10.1126/science.1199705

—. 2010c, ApJS, 188, 405, doi: 10.1088/0067-0049/188/2/405

—. 2011, ApJL, 736, L11, doi: 10.1088/2041-8205/736/1/L11

Abdo, A. A., Ajello, M., Allafort, A., et al. 2013, ApJS, 208, 17, doi: 10.1088/0067-0049/208/2/17

Abdollahi, S., Ackermann, M., Ajello, M., et al. 2017, ApJ, 846, 34, doi: 10.3847/1538-4357/aa8092

Abdollahi, S., Acero, F., Ackermann, M., et al. 2020, The Astrophysical Journal Supplement Series, 247, 33, doi: 10.3847/1538-4365/ab6bcb

Abdollahi, S., Acero, F., Baldini, L., et al. 2022, The Astrophysical Journal Supplement Series, 260, 53, doi: 10.3847/1538-4365/ac6751

Abdollahi, S., Ajello, M., Baldini, L., et al. 2023, ApJS, 265, 31, doi: 10.3847/1538-4365/acbb6a

Abeysekara, A. U., Benbow, W., Bird, R., et al. 2018, ApJL, 867, L19, doi: 10.3847/2041-8213/aae70e

Ackermann, M., Ajello, M., Albert, A., et al. 2013, The Astrophysical Journal, 771, 57, doi: 10.1088/0004-637x/771/1/57

Ackermann, M., Ajello, M., Albert, A., et al. 2014a, Science, 345, 554, doi: 10.1126/science.1253947

—. 2014b, Science, 345, 554, doi: 10.1126/science.1253947

Aharonian, F., Akhperjanian, A. G., Aye, K. M., et al. 2005, A&A, 442, 1, doi: 10.1051/0004-6361:20052983

Ajello, M., Arimoto, M., Axelsson, M., et al. 2019, ApJ, 878, 52, doi: 10.3847/1538-4357/ab1d4e

Albert, A., Alfaro, R., Alvarez, C., et al. 2022, ApJ, 940, 141, doi: 10.3847/1538-4357/ac966a

Arnaud, K. A. 1996, in Astronomical Society of the Pacific Conference Series, Vol. 101, Astronomical Data Analysis Software and Systems V, ed. G. H. Jacoby & J. Barnes, 17

Atwood, W. B., Abdo, A. A., Ackermann, M., et al. 2009, ApJ, 697, 1071, doi: 10.1088/0004-637X/697/2/1071

Aydi, E., Sokolovsky, K., Chomiuk, L., et al. 2020, Direct evidence for shock-powered optical emission in a nova. Nature Astron

Balbo, M., Walter, R., Ferrigno, C., & Bordas, P. 2011, A&A, 527, L4, doi: 10.1051/0004-6361/201015980

Baldini, L., Ballet, J., Bastieri, D., et al. 2021, ApJS, 256, 13, doi: 10.3847/1538-4365/ac072a

Ballet, J., Bruel, P., Burnett, T. H., Lott, B., & The Fermi-LAT collaboration. 2023, arXiv e-prints, arXiv:2307.12546, doi: 10.48550/arXiv.2307.12546

Bates, S. D., Bailes, M., Bhat, N. D. R., et al. 2011, MNRAS, 416, 2455, doi: 10.1111/j.1365-2966.2011.18416.x

Bigongiari, C. 2005, The MAGIC Telescope. https://arxiv.org/abs/astro-ph/0512184

Brill, A. 2023, Self-Supervised Learning for Modeling Gamma-ray Variability in Blazars. https://arxiv.org/abs/2302.07700

Buehler, R., Scargle, J. D., Blandford, R. D., et al. 2012, ApJ, 749, 26, doi: 10.1088/0004-637X/749/1/26

Bühler, R., & Blandford, R. 2014, Reports on Progress in Physics, 77, 066901, doi: 10.1088/0034-4885/77/6/066901

Burns, E., Svinkin, D., Fenimore, E., et al. 2023, ApJL, 946, L31, doi: 10.3847/2041-8213/acc39c

Caliandro, G. A., Cheung, C. C., Li, J., et al. 2015, ApJ, 811, 68, doi: 10.1088/0004-637X/811/1/68

Cao, Z., Aharonian, F., An, Q., et al. 2023, arXiv e-prints, arXiv:2305.17030, doi: 10.48550/arXiv.2305.17030

Chang, Z., Zhang, S., Chen, Y.-P., et al. 2018, Research in Astronomy and Astrophysics, 18, 152, doi: 10.1088/1674-4527/18/12/152

Chernyakova, M., Malyshev, D., van Soelen, B., et al. 2021, Universe, 7, 242, doi: 10.3390/universe7070242

Cheung, C. C., Glanzman, T., & Hill, A. B. 2012a, The Astronomer's Telegram, 4284, 1

Cheung, C. C., Hays, E., Venters, T., Donato, D., & Corbet, R. H. D. 2012b, The Astronomer's Telegram, 4224, 1

Cheung, C. C., Jean, P., Shore, S. N., et al. 2016, The Astrophysical Journal, 826, 142, doi: 10.3847/0004-637x/826/2/142

CHIME/FRB Collaboration, Amiri, M., Andersen, B. C., et al. 2021, ApJS, 257, 59, doi: 10.3847/1538-4365/ac33ab

Ciprini, S., & Fermi-LAT Collaboration. 2012, in American Institute of Physics Conference Series, Vol. 1505, High Energy Gamma-Ray Astronomy: 5th International Meeting on High Energy Gamma-Ray Astronomy, ed. F. A. Aharonian, W. Hofmann, & F. M. Rieger, 697–700

Collaboration, L. 2015, Fermi Large Area Telescope Third Source Catalog. https://arxiv.org/abs/1501.02003

Cutini, S., Bernard, D., & Valverd, J. 2023, The Astronomer's Telegram, 15995, 1

Dinesh, A., Valverde, J., & Garrappa, S. 2023, The Astronomer's Telegram, 15925, 1

Evans, I. N., Primini, F. A., Glotfelty, K. J., et al. 2010, ApJS, 189, 37, doi: 10.1088/0067-0049/189/1/37

Evans, I. N., Primini, F. A., Miller, J. B., et al. 2020, in American Astronomical Society Meeting Abstracts, Vol. 235, American Astronomical Society Meeting Abstracts #235, 154.05

Evans, P. A., Page, K. L., Beardmore, A. P., et al. 2023, MNRAS, 518, 174, doi: 10.1093/mnras/stac2937

Fermi LAT Collaboration, Abdo, A. A., Ackermann, M., et al. 2009, Science, 326, 1512, doi: 10.1126/science.1182174

Franckowiak, A., Jean, P., Wood, M., Cheung, C. C., & Buson, S. 2018, A&A, 609, A120, doi: 10.1051/0004-6361/201731516

H. E. S. S. Collaboration, Abdalla, H., Adam, R., et al. 2020, A&A, 633, A102, doi: 10.1051/0004-6361/201936621

Harris, C., Millman, K., van der Walt, S., et al. 2020, Nature, 585, 357, doi: https://doi.org/10.1038/s41586-020-2649-2

Hays, E., Cheung, T., & Ciprini, S. 2013, The Astronomer's Telegram, 5302, 1

Ho, W. C. G., Ng, C. Y., Lyne, A. G., et al. 2017, MNRAS, 464, 1211, doi: 10.1093/mnras/stw2420

Holder, J., Atkins, R., Badran, H., et al. 2006, Astroparticle Physics, 25, 391–401, doi: 10.1016/j.astropartphys.2006.04.002

Johnson, T. J., Wood, K. S., Kerr, M., et al. 2018, ApJ, 863, 27, doi: 10.3847/1538-4357/aad185

Joye, W. A., & Mandel, E. 2003, in Astronomical Society of the Pacific Conference Series, Vol. 295, Astronomical Data Analysis Software and Systems XII, ed. H. E. Payne, R. I. Jedrzejewski, & R. N. Hook, 489

Koljonen, K. I. I., & Maccarone, T. J. 2017, Monthly Notices of the Royal Astronomical Society, 472, 2181, doi: 10.1093/mnras/stx2106

Krimm, H. A., Holland, S. T., Corbet, R. H. D., et al. 2013, ApJS, 209, 14, doi: 10.1088/0067-0049/209/1/14

Lesage, S., Veres, P., Briggs, M. S., et al. 2023, ApJL, 952, L42, doi: 10.3847/2041-8213/ace5b4

Li, K.-L., & Chomiuk, L. 2016, The Astronomer's Telegram, 9699, 1

Li, K.-L., Chomiuk, L., & Strader, J. 2016, The Astronomer's Telegram, 9736, 1

Li, K. L., Kong, A. K. H., Tam, P. H. T., et al. 2017a, ApJ, 843, 85, doi: 10.3847/1538-4357/aa784e

Li, K. L., Takata, J., Ng, C. W., et al. 2018, ApJ, 857, 123, doi: 10.3847/1538-4357/aab848

Li, K.-L., Metzger, B. D., Chomiuk, L., et al. 2017b, Nature Astronomy, 1, 697, doi: 10.1038/s41550-017-0222-1

Lien, A., Sakamoto, T., Barthelmy, S. D., et al. 2016, ApJ, 829, 7, doi: 10.3847/0004-637X/829/1/7

Massaro, E., Maselli, A., Leto, C., et al. 2015, Ap&SS, 357, 75, doi: 10.1007/s10509-015-2254-2

Massaro, F., D'Abrusco, R., Tosti, G., et al. 2012, The Astrophysical Journal, 750, 138, doi: 10.1088/0004-637x/750/2/138

Metzger, B. D., Caprioli, D., Vurm, I., et al. 2016, MNRAS, 457, 1786, doi: 10.1093/mnras/stw123

Minkowski, R. 1942, ApJ, 96, 199, doi: 10.1086/144447

Mirabel, I. 2012, Science, 335, 175

Munari, U., Hambsch, F. J., & Frigo, A. 2017, MNRAS, 469, 4341, doi: 10.1093/mnras/stx1116

Nasa High Energy Astrophysics Science Archive Research Center (Heasarc). 2014, HEAsoft: Unified Release of FTOOLS and XANADU, Astrophysics Source Code Library, record ascl:1408.004. http://ascl.net/1408.004

Nelson, T., Mukai, K., Li, K.-L., et al. 2019, ApJ, 872, 86, doi: 10.3847/1538-4357/aafb6d

Nolan, P. L., Abdo, A. A., Ackermann, M., et al. 2012, ApJS, 199, 31, doi: 10.1088/0067-0049/199/2/31

Oh, K., Koss, M., Markwardt, C. B., et al. 2018, ApJS, 235, 4, doi: 10.3847/1538-4365/aaa7fd

Otero-Santos, J., Peñil, P., Acosta-Pulido, J. A., et al. 2023, MNRAS, 518, 5788, doi: 10.1093/mnras/stac3142

Peñil, P., Ajello, M., Buson, S., et al. 2022, arXiv e-prints, arXiv:2211.01894, doi: 10.48550/arXiv.2211.01894

Pittori, C., Tavani, M., Bulgarelli, A., et al. 2023, The Astronomer's Telegram, 15952, 1

Prokhorov, D. A., & Moraghan, A. 2022, Monthly Notices of the Royal Astronomical Society, 519, 2680, doi: 10.1093/mnras/stac3453

R Core Team. 2023, R: A Language and Environment for Statistical Computing, R Foundation for Statistical Computing, Vienna, Austria

Scargle, J. D., Norris, J. P., Jackson, B., & Chiang, J. 2013, The Astrophysical Journal, 764, 167, doi: 10.1088/0004-637x/764/2/167

Striani, E., Tavani, M., Piano, G., et al. 2011, ApJL, 741, L5, doi: 10.1088/2041-8205/741/1/L5

Striani, E., Tavani, M., Vittorini, V., et al. 2013, ApJ, 765, 52, doi: 10.1088/0004-637X/765/1/52

Suvorov, A. G., & Glampedakis, K. 2022, The Astrophysical Journal, 940, 128

Tam, P. H. T., He, X. B., Pal, P. S., & Cui, Y. 2018, ApJ, 862, 165, doi: 10.3847/1538-4357/aacf00

Tam, P. H. T., Huang, R. H. H., Takata, J., et al. 2011, ApJL, 736, L10, doi: 10.1088/2041-8205/736/1/L10

Tavani, M., Bulgarelli, A., Vittorini, V., et al. 2011, Science, 331, 736, doi: 10.1126/science.1200083

Taylor, M. B. 2005, in Astronomical Society of the Pacific Conference Series, Vol. 347, Astronomical Data Analysis Software and Systems XIV, ed. P. Shopbell, M. Britton, & R. Ebert, 29

The Astropy Collaboration, Robitaille, Thomas P., Tollerud, Erik J., et al. 2013, A&A, 558, A33, doi: 10.1051/0004-6361/201322068

Theureau, G., Parent, D., Cognard, I., et al. 2011, A&A, 525, A94, doi: 10.1051/0004-6361/201015317

Torres, D. F., Rea, N., Esposito, P., et al. 2011, The Astrophysical Journal, 744, 106, doi: 10.1088/0004-637x/744/2/106

Urry, M. 1999, in Astronomical Society of the Pacific Conference Series, Vol. 159, BL Lac Phenomenon, ed. L. O. Takalo & A. Sillanpää, 3

van Kerkwijk, M. H., Charles, P. A., Geballe, T. R., et al. 1992, Nature, 355, 703, doi: 10.1038/355703a0

von Kienlin, A., Meegan, C. A., Paciesas, W. S., et al. 2020, The Astrophysical Journal, 893, 46, doi: 10.3847/1538-4357/ab7a18

Wang, N., Johnston, S., & Manchester, R. N. 2004, Monthly Notices of the Royal Astronomical Society, 351, 599, doi: 10.1111/j.1365-2966.2004.07806.x

Webb, N. A., Coriat, M., Traulsen, I., et al. 2020, A&A, 641, A136, doi: 10.1051/0004-6361/201937353

Wenger, M., Ochsenbein, F., Egret, D., et al. 2000, A&AS, 143, 9, doi: 10.1051/aas:2000332